Limnol. Oceanogr., 58(4), 2013, 1312–1328

doi:10.4319/lo.2013.58.4.1312

Biological production rates off the Southern California coast estimated from triple O_2 isotopes and O_2 : Ar gas ratios

David R. Munro,[1,a,*] Paul D. Quay,[1] Laurie W. Juranek,[2] and Ralf Goericke[3]

[1] School of Oceanography, University of Washington, Seattle, Washington
[2] College of Earth, Ocean, and Atmospheric Sciences, Oregon State University, Corvallis, Oregon
[3] Scripps Institution for Oceanography, University of California, San Diego, California

Abstract

The isotopic composition of dissolved O_2 ($^{17}\Delta$) and the biological O_2 saturation from O_2 : Ar ratios were measured in the surface ocean during six cruises off the coast of southern California from November 2005 to August 2008 to determine rates of gross oxygen production (GOP), net oxygen production (NOP), and the NOP : GOP ratio (a measure of potential export efficiency). In the mixed layer, $^{17}\Delta$ of dissolved O_2 ($^{17}\Delta_{diss}$) ranged from 24 to 108 per meg and biological O_2 saturation ranged from 101% to 113% for all regions and cruises. Mixed-layer $^{17}\Delta$-GOP ranged from 49 ± 23 mmol O_2 m^{-2} d^{-1} to 533 ± 185 mmol O_2 m^{-2} d^{-1} with an annual mean for the California Cooperative Oceanic Fisheries Investigations (CalCOFI) grid of 151 ± 59 mmol O_2 m^{-2} d^{-1}. Mixed-layer O_2 : Ar-NOP ranged from 8 ± 6 mmol O_2 m^{-2} d^{-1} to 135 ± 31 mmol O_2 m^{-2} d^{-1} with an annual mean of 25 ± 8 mmol O_2 m^{-2} d^{-1}, implying that the CalCOFI grid is autotrophic year-round. $^{17}\Delta$-GOP estimates were consistently greater than on-deck incubation-based ^{14}C-primary production (^{14}C-PP) by a factor of 5.6 ± 0.4 and greater than satellite PP estimates by a factor of 3.5 ± 0.3 (mmol O_2 : mmol C). The $^{17}\Delta$-GOP to ^{14}C-PP factor was twice the expected factor of 2.7 determined from comparisons of incubation-based ^{18}O-GOP and ^{14}C-PP. The annual mean NOP : GOP ratio was 0.16 ± 0.06, suggesting a potential export efficiency that is surprisingly similar to the open ocean using comparable methods.

The rate of aquatic primary production (PP) is of fundamental importance to understanding of ocean ecosystems, marine biogeochemical cycling, and predictions of how ocean ecosystems will respond to climate change. Although satellite sensors and algorithms provide quantitative estimates of ocean chlorophyll and PP at spatial and temporal resolution not achievable with ship-based methods, satellite-based global PP estimates differ by a factor of two and divergence between methods is particularly great in high-chlorophyll regions such as the continental margins (Carr et al. 2006). Ultimately, the test of satellite-based PP methods is validation by direct observation. Unfortunately, there is no absolute method to measure aquatic PP, leading to considerable debate regarding the accuracy and interpretation of available PP methods.

Since its introduction over 5 decades ago, the ^{14}C incubation approach (^{14}C-PP) has been the most widely used PP method in oceanography. The enormous data set of ^{14}C-PP measurements has contributed greatly to our understanding of oceanic productivity, but fundamental questions remain with regard to its accuracy (Marra 2002). The ^{14}C-PP method, like most PP methods, is an in vitro approach and as such there is inherent uncertainty as to whether rates determined inside a bottle accurately reflect in situ rates. Other specific methodological concerns include differences between on-deck and in situ bottle incubations, duration of incubation (generally 6–24 h), recycling of respired CO_2, recycling of labeled organic material, and production of labeled (unmeasured) dissolved organic carbon (DOC; Marra 2002). Direct comparisons with O_2-based in vitro approaches, including ^{18}O incubations and O_2 light and dark incubations, have helped address some of the ^{14}C-PP measurement ambiguity such that under most conditions 24 h ^{14}C-PP incubations are assumed to represent net primary production (NPP), which is also the parameter estimated by satellite-based approaches (Marra 2002). Bottle effects during incubation have been impossible to quantify because of a lack of a PP reference standard.

The triple O_2 isotope method for measuring aquatic gross O_2 production ($^{17}\Delta$-GOP) is based on precise measurement of the natural ^{17}O : ^{16}O and ^{18}O : ^{16}O ratios of mixed-layer dissolved O_2 (Luz and Barkan 2000). The $^{17}\Delta$-GOP method provides several key advantages over traditional PP methods. (1) It is based on a mixed-layer O_2 budget, and is not an incubation-based approach; thus, it avoids the unknowns inherent to in vitro methodologies. (2) Very little sample processing is required aboard ship, which greatly expands measurement capability. (3) The $^{17}\Delta$-GOP method integrates over the residence time of O_2 in the mixed layer (typically 1 week in the coastal ocean), which increases the chances of capturing productivity events missed by short-duration incubation experiments. (4) Measurement of the ratio of dissolved O_2 and Ar gases (O_2 : Ar) made on the same sample provides a contemporaneous estimate of net O_2 production (NOP), which yields a rate of net carbon production (NCP) that integrates both particulate organic carbon (POC) export and net DOC production. Combining $^{17}\Delta_{diss}$ and O_2 : Ar measurements provides a nonincubation-based measure of potential

* Corresponding author: david.munro@colorado.edu

[a] Institute of Arctic and Alpine Research, University of Colorado, Boulder, Colorado

export efficiency (NOP : GOP), where both numerator and denominator are integrated over the same timescale and measured in terms of O_2.

The disadvantages of the $^{17}\Delta$-GOP method include significant uncertainty in GOP estimates due to uncertainty in the gas exchange parameterization and $^{17}\Delta$ measurement precision. In some situations, the mixed-layer budget must include terms for horizontal advection, vertical advection, and mixed-layer deepening (i.e., entrainment). The $^{17}\Delta$-GOP and O_2 : Ar-NOP methods integrate through the mixed layer and can miss a significant fraction of the productivity when the mixed-layer depth is substantially shallower than the photic zone (Luz and Barkan 2009). Another caveat is the ambiguity in relating photosynthetic O_2 production to carbon fixation (Zehr and Kudela 2009). Because all available PP methods come with significant limitations, we emphasize the importance of applying multiple PP methods to a given study region to more accurately characterize PP variability.

Several previous studies have employed the $^{17}\Delta$-GOP method in open-ocean environments, including at the Bermuda Atlantic Time-Series (BATS; Luz and Barkan 2000, 2009), the Hawaii Ocean Time-Series (HOT; Juranek and Quay 2005; Quay et al. 2010), the subtropical North and South Pacific (Juranek and Quay 2010), the equatorial Pacific (Juranek and Quay 2010; Stanley et al. 2010), the subarctic North Atlantic (Quay et al. 2012), and the Southern Ocean (Hendricks et al. 2004; Reuer et al. 2007). The only previous studies to employ the $^{17}\Delta$-GOP method in the coastal ocean were conducted in Sagami Bay off the coast of Japan (Sarma et al. 2008).

Eastern Boundary Current (EBC) systems, such as the California Current System (CCS), are among the most biologically productive oceanic environments, accounting for 35% of global annual wild fish catch despite covering just 1% of the ocean surface area (Kudela et al. 2008). Coastal regions, generally, are important for the export of biologically fixed carbon to the deep ocean and sediments; recent estimates suggest that 30–50% of global carbon export may occur along continental margins (Dunne et al. 2007). The CCS is highly sensitive to climate variability with recent studies demonstrating significant physical and ecological responses to both the El Niño-Southern Oscillation (Kahru and Mitchell 2002) and the Pacific Decadal Oscillation (Chhak and Di Lorenzo 2007). Potential effects of future climate change have been hypothesized, including intensification of coastal upwelling in response to increased upwelling-favorable wind stress (Bakun 1990) and increased stratification associated with surface warming (Di Lorenzo et al. 2005). Over the past decade, PP in the CCS and other EBC systems appears to be increasing (Kahru et al. 2009), accompanied in many regions by decreasing O_2 concentrations at depth (Bograd et al. 2008). Clearly, accurate PP measurements are critical to understanding links between PP, climate variability, air–sea CO_2 flux, hypoxia, and productivity at higher trophic levels.

The California Cooperative Oceanic Fisheries Investigations (CalCOFI) program was initiated in 1949 in response to the collapse of the sardine fishery and is one of the longest running oceanographic sampling programs in existence. ^{14}C-PP measurements began in 1984 and represent one of the most extensive oceanic PP data sets available. The CalCOFI program provides an excellent setting in which to apply the $^{17}\Delta$-GOP method because of the opportunity for direct comparison with ^{14}C-PP and regional satellite-based PP estimates (Kahru et al. 2009).

The objectives of this study are (1) to determine seasonal and spatial variability in PP and NCP in the CCS using two nonincubation methods ($^{17}\Delta$-GOP and O_2 : Ar-NOP), (2) to compare $^{17}\Delta$-GOP and O_2 : Ar-NOP estimates with concurrent ^{14}C-PP and satellite-based PP estimates, and (3) to determine variability in the potential export ratio, NOP : GOP, independent of incubation methods. This study represents the most extensive application of the $^{17}\Delta$-GOP and O_2 : Ar-NOP methods in an EBC system to date.

Methods

Study area—The CalCOFI grid currently includes 75 stations spread over 6 lines perpendicular to the Southern California coast, extending southwest from Point Arguello to San Diego (Fig. 1). Station spacing ranges from < 20 km close to shore to ~ 75 km offshore. Cruises are conducted quarterly (typically in January, April, July or August, and October or November). Individual stations are typically referred to by a line and station number (e.g., 77.100 represents Sta. 100, the outermost station, on line 77, the northernmost line).

Samples for O_2 isotopes and O_2 : Ar were collected during six CalCOFI cruises from November 2005 to August 2008. We refer to each cruise using the standard CalCOFI notation, whereby the first two digits refer to the year, the third and fourth digits refer to the month, and the succeeding letters refer to the research vessel (i.e., 0511NH refers to a cruise of the R/V *New Horizon* in November 2005; other vessels include the R/V *Roger Revelle* and the R/V *David Starr Jordan*). We group stations into four regions based on physical setting and historical productivity rates (Fig. 1). The North Inshore region (Region 1) encompasses the high historical PP rates associated with the persistent upwelling feature off Point Conception. The South Inshore region (Region 2) includes the Southern California Bight, which has markedly lower productivity in comparison with other regions inshore of the California Current along the West Coast (Eppley 1992). The California Current region (Region 3) is distinguished by high equator-ward transport via the California Current. The Offshore region (Region 4) has historical productivity rates that approach those of the oligotrophic subtropical North Pacific.

$^{17}\Delta$-GOP, O_2 : Ar-NOP, and NOP : GOP methods—The details of the $^{17}\Delta$-GOP method have been described previously (Luz and Barkan 2000; Hendricks et al. 2004; Juranek and Quay 2005) and only the fundamentals of the method are summarized here. The method is based on a small but measureable isotopic anomaly, which differentiates atmospheric O_2 from O_2 produced during photosynthesis. The O_2 isotopic anomaly is expressed using $^{17}\Delta$ notation (Luz and Barkan 2011):

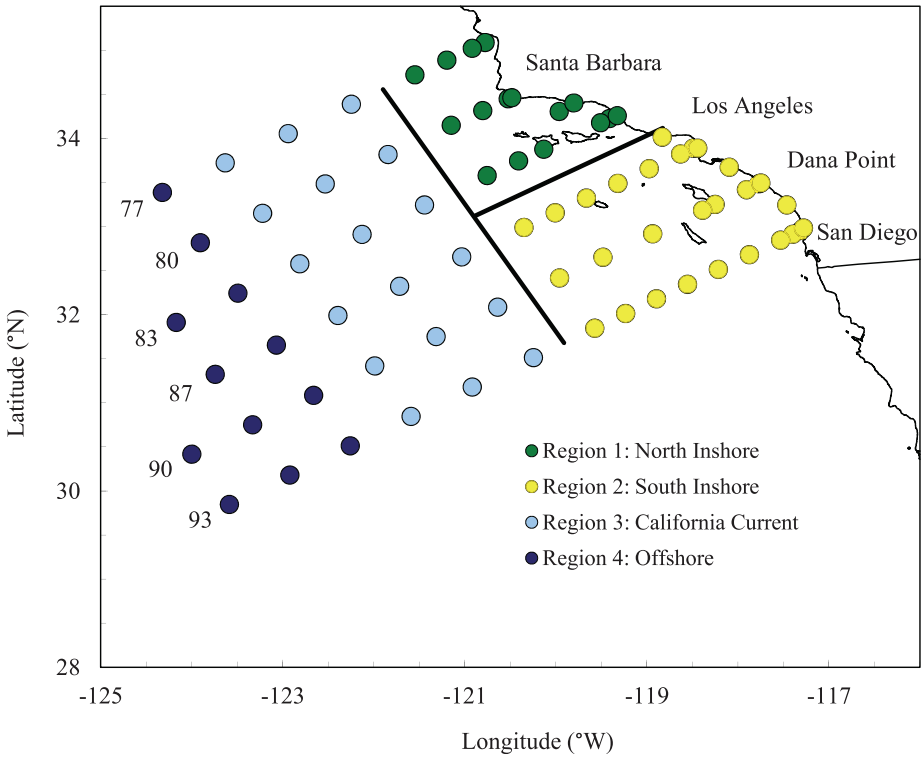

Fig. 1. CalCOFI station positions with locations of standard stations and Southern California Coastal Ocean Observing System (SCCOOS) stations (circles). Region 1 (North Inshore) is green. Region 2 (South Inshore) is yellow. Region 3 (California Current) is light blue. Region 4 (Offshore) is dark blue. Alongshore transports were calculated across the line separating CalCOFI lines 83 and 87 between Regions 1 and 2. Offshore and onshore transports were calculated across the line separating Sta. 60 and 70 between Regions 1, 3 and Regions 2, 3.

$$^{17}\Delta = (\ln[\delta^{17}O/1000+1] - 0.518 \times \ln[\delta^{18}O/1000+1]) \times 10^6 \quad (1)$$

where $\delta^{17}O$ and $\delta^{18}O$ (in ‰) represents $(R_{sample} : R_{standard} - 1) \times 1000$ and $R = {}^{17}O : {}^{16}O$ or ${}^{18}O : {}^{16}O$ for O_2. The value of 0.518 represents the ratio of ${}^{17}O : {}^{18}O$ fractionation for respiration empirically measured for plankton, microbes, and plants (Luz and Barkan 2011). $^{17}\Delta$ is reported in units of per meg (10^6) rather than per mil relative to atmospheric O_2 (0 per meg). The $^{17}\Delta$ of dissolved O_2 in seawater ($^{17}\Delta_{diss}$) ranges from close to the atmospheric end member to 249 ± 15 per meg for purely photosynthetic O_2 ($^{17}\Delta_p$) on the high end (Luz and Barkan 2000). The $^{17}\Delta$ of atmospheric O_2 dissolved in seawater ($^{17}\Delta_{eq}$) is temperature-dependent and has been estimated empirically by Luz and Barkan (2009; $^{17}\Delta_{eq} = 0.6 \times t + 1.8$) where t is temperature in °C.

$^{17}\Delta_{diss}$ is thus a direct measure of the proportion of photosynthetic vs. atmospheric O_2. To calculate the GOP rate from measured $^{17}\Delta_{diss}$ requires setting up mixed-layer O_2 budgets for each isotopologue of O_2 (mass 32, 33, and 34) as described by Hendricks et al. (2004). Assuming steady state, an equation for GOP integrated through the mixed layer can be derived (Luz and Barkan 2000):

$$GOP = K_g \times C_{sat} \times \left({}^{17}\Delta_{diss} - {}^{17}\Delta_{eq}\right) / \left({}^{17}\Delta_p - {}^{17}\Delta_{diss}\right) \quad (2)$$

where K_g (m d^{-1}) is the gas transfer velocity based on an empirically determined function of wind speed specific to O_2, and C_{sat} (mmol m^{-3}) is the concentration of O_2 at saturation. Equation 2 can be modified to include advective transport terms in regions where horizontal or vertical advection rates are high and/or horizontal or vertical $^{17}\Delta_{diss}$ gradients are large (e.g., as done for the equatorial Pacific by Juranek and Quay 2010), or during periods of mixed-layer deepening when subsurface water with high $^{17}\Delta_{diss}$ is entrained into the mixed layer (Quay et al. 2010).

Ar acts as a biologically inert analog for O_2; therefore, the dissolved $O_2 : Ar$ gas ratio divided by the $O_2 : Ar$ ratio expected at equilibrium with air gives a measure of biological O_2 saturation (i.e., $[O_2 : Ar]_{meas}/[O_2 : Ar]_{sat}$; Craig and Hayward 1987). Mixed-layer steady-state O_2 and Ar budgets have been used to derive an expression for NOP (Emerson et al. 1997):

$$NOP = K_g \times C_{sat} \times \left(\left[(O_2 : Ar)_{meas} / (O_2 : Ar)_{sat} \right] - 1 \right) \quad (3)$$

where $(O_2 : Ar)_{sat}$ depends on measured temperature and salinity (Garcia and Gordon 1992; Hamme and Emerson 2004). This expression, like Eq. 2, ignores advective transport terms.

The NOP : GOP ratio, a measure of biological production efficiency, results from the combination of Eqs. 2 and 3 to yield

$$\mathrm{NOP:GOP} = \left(\left[(\mathrm{O_2:Ar})_{\mathrm{meas}}/(\mathrm{O_2:Ar})_{\mathrm{sat}}\right]-1\right) \times \left({}^{17}\Delta_{\mathrm{diss}} - {}^{17}\Delta_{\mathrm{p}}\right)/\left({}^{17}\Delta_{\mathrm{eq}} - {}^{17}\Delta_{\mathrm{diss}}\right) \quad (4)$$

again assuming steady state and ignoring advective terms. Importantly, NOP:GOP is essentially independent of gas exchange and its associated uncertainty. In addition, both numerator and denominator are measured in units of O_2 and integrated over the same time period, avoiding the uncertainty of converting measurements in different units that integrate over different time and space scales.

GOP and NOP including advection—Mixed-layer budgets for the two stable isotopologues of O_2 of interest (i.e., $^{16}O^{17}O$ and $^{16}O^{18}O$) are constructed following Hendricks et al. (2004):

$$\begin{aligned} \mathrm{h}\times \mathrm{d}(\mathrm{C_{ml}}\times \mathrm{X_{ml}})/\mathrm{dt} = {} & \mathrm{GOP}\times \mathrm{X_p} - \mathrm{R}\times \alpha_{\mathrm{r}} \times \mathrm{X_{ml}} \\ & + \mathrm{K_g}\times \alpha_{\mathrm{g}}(\mathrm{C_{sat}}\times \mathrm{X_{air}}\times \alpha_{\mathrm{sol}} - \mathrm{C_{ml}}\times \mathrm{X_{ml}}) \\ & + \mathrm{h}\times (\mathrm{u}/\mathrm{L_x})\times (\mathrm{C_x}\times \mathrm{X_x} - \mathrm{C_{ml}}\times \mathrm{X_{ml}}) \\ & + \mathrm{h}\times (\mathrm{v}/\mathrm{L_y})\times (\mathrm{C_y}\times \mathrm{X_y} - \mathrm{C_{ml}}\times \mathrm{X_{ml}}) \\ & + \mathrm{w}\times (\mathrm{C_z}\times \mathrm{X_z} - \mathrm{C_{ml}}\times \mathrm{X_{ml}}) \end{aligned} \quad (5)$$

where h (m) is the mixed-layer depth; R is the respiration rate (mmol O_2 m^{-2} d^{-1}); u and v represent zonal and alongshore velocities (m d^{-1}); w represents upwelling rate (m d^{-1}); C_{ml} represents the mixed-layer O_2 concentration (mmol O_2 m^{-3}); C_x and C_y represent the upstream O_2 concentrations for zonal and alongshore transports (mmol O_2 m^{-3}); C_z represents the O_2 concentration below the mixed layer (mmol O_2 m^{-3}); L_x and L_y represent the horizontal length scales over which the gradients in O_2 are considered (m); X_{ml} represents the isotope ratio $^{17}O:^{16}O$ or $^{18}O:^{16}O$ of mixed-layer O_2; X_p represents the isotopic composition of photosynthetic O_2; X_x, X_y, and X_z represent the isotopic composition of upstream O_2 and O_2 below the mixed layer; α_r and α_g represent the kinetic fractionation effects due to respiration and gas exchange, respectively, and α_{sol} is the O_2 solubility equilibrium fractionation effect. $d(C_{ml} \times X_{ml})/dt$ is the rate of change for an O_2 isotopologue in the mixed layer (equal to zero at steady state; mmol O_2 m^{-3} d^{-1}). Horizontal gradients were calculated between the four regions in the CalCOFI grid described above (Fig. 1). Combining the equations for $^{16}O^{17}O$ and $^{16}O^{18}O$ expressed in terms of $^{17}\Delta$ and solving for GOP (assuming that respiration has no effect on mixed-layer $^{17}\Delta_{diss}$ as discussed above) yields

$$\begin{aligned} \mathrm{GOP} = {} & [\mathrm{K_g}\times \mathrm{C_{sat}}\times \left({}^{17}\Delta_{\mathrm{diss}} - {}^{17}\Delta_{\mathrm{eq}}\right) \\ & + \mathrm{h}\times (\mathrm{u}/\mathrm{L_x})\times \left({}^{17}\Delta_{\mathrm{diss}} - {}^{17}\Delta_{\mathrm{x}}\right) \\ & + \mathrm{h}\times (\mathrm{v}/\mathrm{L_y})\times \left({}^{17}\Delta_{\mathrm{diss}} - {}^{17}\Delta_{\mathrm{y}}\right) \\ & + \mathrm{w}\times \left({}^{17}\Delta_{\mathrm{z}} - {}^{17}\Delta_{\mathrm{eq}}\right)]/\left({}^{17}\Delta_{\mathrm{p}} - {}^{17}\Delta_{\mathrm{diss}}\right) \end{aligned} \quad (6)$$

Recently, the equation to calculate GOP rates from dissolved O_2 isotope measurements has been improved to allow direct calculation from the $^{18}O:^{16}O$ and $^{17}O:^{16}O$ ratios rather than in terms of $^{17}\Delta$ (Luz and Barkan 2011; Prokopenko et al. 2011). We use the revised approach outlined by Luz and Barkan (2011) with additional terms for horizontal and vertical advection as included in Eqs. 5 and 6; for this study, the revised approach yields GOP rates that are within 5% (for individual regions) of rates calculated using Eq. 6.

Similarly, the expression for NOP can be modified to include horizontal and vertical advection terms as follows:

$$\begin{aligned} \mathrm{NOP} = {} & \mathrm{K_g}\times \mathrm{C_{sat}}\times ((\mathrm{O_2:Ar})_{\mathrm{bio\_ml}} - 1) \\ & + \mathrm{h}\times (\mathrm{u}/\mathrm{L_x})\times \mathrm{C_x}\times (((\mathrm{O_2:Ar})_{\mathrm{bio\_ml}}/(\mathrm{O_2:Ar})_{\mathrm{bio\_x}}) - 1) \\ & + \mathrm{h}\times (\mathrm{v}/\mathrm{L_y})\times \mathrm{C_y}\times (((\mathrm{O_2:Ar})_{\mathrm{bio\_ml}}/(\mathrm{O_2:Ar})_{\mathrm{bio\_y}}) - 1) \\ & + \mathrm{w}\times \mathrm{C_z}\times (((\mathrm{O_2:Ar})_{\mathrm{bio\_ml}}/(\mathrm{O_2:Ar})_{\mathrm{bio\_z}}) - 1) \end{aligned} \quad (7)$$

where $(O_2:Ar)_{bio}$ represents the biological O_2 saturation in the mixed layer (ml) and for water transported zonally (x), alongshore (y), and via upwelling (z).

To determine the likelihood that steady-state conditions were met for the GOP and NOP calculation, we compared surface-water residence times with the dissolved O_2 residence times in the four regions described above. For all regions, the O_2 replenishment time due to air–sea exchange was 4–8 d, which was a result of mixed-layer depths of 25–35 m divided by a K_g of 3–6 m d^{-1}. In comparison, for the North Inshore region the average water residence time was 11 d based on an average current velocity of 15 cm s^{-1} calculated from geostrophic and Ekman transports. Similar calculations yielded water residence times of 26, 17, and 26 d for the South Inshore, California Current, and Offshore regions, respectively. For all regions, residence times for water are 2–5× greater than residence times for O_2, suggesting that mixed-layer O_2, $^{17}\Delta_{diss}$, and $O_2:Ar$ approach a steady-state balance between biological production, air–sea gas exchange, and advection within each region.

PP terminology and conversions—The terminology used to describe PP rates can be confusing due in part to differences in what various methods actually measure. For clarity, we define the following terms. Gross O_2 production (GOP) refers to the amount of O_2 production during photosynthesis and is typically expressed as a vertically integrated daily rate (mmol O_2 m^{-2} d^{-1}). GOP can be determined by both $^{17}\Delta$ measurements as reported here, or by $H_2{}^{18}O$ incubation experiments (^{18}O-GOP).

Estimates from two commonly used satellite-based PP models, the Vertically Generalized Productivity Model (VGPM; Behrenfeld and Falkowski 1997) and the Carbon based Productivity Model (CbPM; Westberry et al. 2008), were acquired from the Ocean Productivity Group at Oregon State University (http://web.science.oregonstate.edu/ocean.productivity/custom.php) for comparison with $^{17}\Delta$-GOP and ^{14}C-PP measurements. Although ^{14}C-PP and most satellite methods are assumed to approximate net

autotrophic primary production (NPP), we use the method name to define the measured rate (e.g., ^{14}C-PP, VGPM-PP for the Vertically Generalized Productivity Model, and CbPM-PP for the Carbon based Productivity Model). Rates estimated using triple O_2 isotope composition will similarly be defined by $^{17}\Delta$-GOP. Because $^{17}\Delta$-GOP is estimated using a mixed-layer budget for O_2 and O_2 isotopologues, we determine the mixed-layer fraction of ^{14}C-PP for comparisons between methods. The ^{14}C-PP mixed-layer fraction can also be used to extrapolate mixed-layer $^{17}\Delta$-GOP estimates to the photic zone, where it exceeds the mixed-layer depth (i.e., by dividing mixed-layer $^{17}\Delta$-GOP by the mean mixed-layer fraction of ^{14}C-PP for each region and cruise).

Lastly, net O_2 production (NOP) equals GOP minus community respiration and at steady state is equal to the amount of PP available for export (mmol O_2 m^{-2} d^{-1}), whether by sinking flux, conversion to dissolved organic matter, or transfer to higher trophic levels. NOP is converted to NCP (mg C m^{-2} d^{-1}) using a photosynthetic quotient for new production of 1.4 (Laws 1991). As mentioned above, our NCP rates integrate both POC export and net DOC production. The NOP : GOP ratio can be related to the ratio of new production to NPP (i.e., the f-ratio) by assuming a photosynthetic quotient of 1.4 for new production and assuming a constant ratio of GOP : NPP of 2.7, as determined from comparisons of ^{14}C-PP and ^{18}O-GOP (Marra 2002).

^{14}C-PP measurement—A detailed sampling procedure for CalCOFI ^{14}C-PP and other hydrographic sampling techniques is described on the CalCOFI website (http://www.calcofi.org/field-program/rosette-sampling.html); several important aspects of the procedure are relevant for this study. ^{14}C-PP samples are collected from a mid-morning cast each day at six depths determined by the photic zone depth and depth of the chlorophyll maximum. The deepest ^{14}C-PP depth receives 0.2–0.5% of the surface irradiance. Incubations are conducted over half a light cycle from local apparent noon to sunset in on-deck incubators cooled with surface seawater and with neutral-density screens to simulate in situ light conditions at each depth. Eppley (1992) used comparisons of concurrent ^{14}C-PP_{24h} to half-day ^{14}C-PP_{6h} conducted by CalCOFI and the Southern California Bight study to estimate a scaling factor of 1.81 (i.e., multiplying ^{14}C-PP_{6h} by 1.81 provides an estimate of ^{14}C-PP_{24h}). ^{14}C-PP rates reported by CalCOFI were multiplied by 1.81 to estimate ^{14}C-PP_{24h} and to provide a more useful comparison with other PP estimates.

Estimating rates of gas exchange and advection—To calculate K_g necessary for GOP and NOP estimates, we used wind-speed data (referenced to a height of 10 m) from the SeaWinds instrument on the QuikSCAT satellite processed daily on $0.5^\circ \times 0.5^\circ$ fields. K_g was calculated using the parameterization of Nightingale et al. (2000). The daily weighting approach of Reuer et al. (2007) was used to calculate averaged K_g values representative of the residence time of O_2 in the mixed layer.

Upwelling due to wind stress curl (curl-driven upwelling) can be comparable to coastal upwelling as a source of nutrients in the CalCOFI region (Rykaczewski and Checkley 2008). QuikSCAT wind stress was calculated using the equations of Large et al. (1994) and used to calculate curl-driven upwelling rates (w_{curl}) for every region sampled for O_2 isotopic composition and O_2 : Ar.

Coastal upwelling rates (w_{coast}) for the nearshore regions of Regions 1 and 2 were calculated using the offshore Ekman transport from National Data Buoy Center winds; buoys 46023 and 46063 were used for the North Inshore region and buoy 46025 was used for the South Inshore region. Upwelling rates based on buoy winds agree closely with estimates based on QuikSCAT winds.

Horizontal current velocities were determined from calculations of geostrophic velocities (relative to 500 m) using dynamic height data (http://www.calcofi.org/data/x-btldata.html); surface-layer Ekman velocities were calculated from QuikSCAT wind stress. Geostrophic velocities were extrapolated into depths shallower than 500 m using the approach of Reid and Mantyla (1976). A rotated coordinate system was used such that 'u' represents velocity parallel to CalCOFI lines 77–93 and 'v' represents velocity perpendicular to the CalCOFI lines (Fig. 1).

Sample collection and analytical methods for O_2 isotope and O_2 : Ar measurements—Samples for $^{17}\Delta_{diss}$ and O_2 : Ar were collected from Niskin bottles within the mixed layer (typically < 25 m) at 15–50 stations per cruise. Depth profiles (four to seven depths) were collected at three to five stations per cruise to characterize the photic zone and upper aphotic zone.For O_2 isotope and O_2 : Ar samples, 150–250 mL of seawater was collected in pre-evacuated bottles (300–500 mL) poisoned with 200 μL of saturated $HgCl_2$ solution following the protocol of Juranek and Quay (2005). In the lab, samples were equilibrated at room temperature for 12–24 h and afterward seawater was removed by vacuum. After equilibration, samples were typically stored for several weeks (never > 6 months) before mass spectrometer analysis. Bottle sidearms were filled with seawater at the time of collection and then with CO_2 after equilibration to limit air contamination.

Mass spectrometer measurement procedure has been described in Juranek and Quay (2005). Internal precision based on standard error of the mean (SEM) of 75 paired measurements is as follows: $\pm$ 7 per meg for $^{17}\Delta$, 0.003‰ for δ^{18}O, and 0.007‰ for δ^{17}O. $^{17}\Delta_{diss}$ of each sample was corrected for variation in O_2 : Ar. Final $^{17}\Delta_{diss}$ and O_2 : Ar values are reported vs. air using a lab gas standard calibrated daily against air. The overall measurement uncertainty was calculated from 39 replicate sample pairs collected from the same Niskin bottle where the mean standard deviation (SD) for all replicates was $\pm$ 9 per meg for $^{17}\Delta_{diss}$ and $\pm$ 0.1% for biological O_2 saturation.

Results

$^{17}\Delta$-GOP estimates—Mean mixed-layer $^{17}\Delta_{diss}$ for each of the four regions calculated for each cruise ranged from 24 $\pm$ 3 to 108 $\pm$ 12 per meg (Table 1), where uncertainty represents the SEM of all mixed-layer samples collected in a given region during each cruise. Depth profiles typically

Table 1. Seasonal range and annual mean values of mixed-layer $^{17}\Delta_{diss}$ and biological O_2 saturation for each region; $^{17}\Delta_{diss}$ is relative to atmospheric O_2. Uncertainty is calculated as the standard error of the mean (SEM) for all mixed-layer values in a given region during each cruise (i.e., SD $\times$ $n^{-0.5}$). Uncertainty in the annual mean represents the mean SEM for each region for all cruises.

	Seasonal range $^{17}\Delta_{diss}$ (in per meg)	Annual mean $^{17}\Delta_{diss}$ (in per meg)	Seasonal range biological O_2 saturation	Annual mean biological O_2 saturation
Region 1: North Inshore	68±6 to 108±12	87±7	1.037±0.005 to 1.127±0.024	1.069±0.012
Region 2: South Inshore	58±5 to 91±2	68±5	1.013±0.005 to 1.062±0.006	1.038±0.007
Region 3: California Current	33±2 to 55±16	44±5	1.008±0.002 to 1.030±0.002	1.019±0.003
Region 4: Offshore	24±3 to 43±7	34±4	1.008±0.001 to 1.017±0.001	1.013±0.002
CalCOFI grid	44±3 to 60±3	53±5	1.016±0.002 to 1.040±0.005	1.028±0.005

show $^{17}\Delta_{diss}$ maxima (up to 139 per meg) beneath the mixed layer within the photic zone that are most pronounced during summer and autumn (Fig. 2) in oligotrophic regions of the CalCOFI grid including the Southern California Bight, and in the aphotic zone, $^{17}\Delta_{diss}$ decreases to a mean of 74 ± 13 per meg (n = 5) at 200–300 m. Depth profiles for regions of active upwelling show little vertical variability (Fig. 2). Mixed-layer $^{17}\Delta_{diss}$ was highest in the North Inshore region (annual mean = 87 ± 7 per meg) and lowest in the Offshore region (annual mean = 34 ± 4 per meg; Table 1; Fig. 3). Uncertainty in the annual mean represents the mean SEM in each region for all cruises. Seasonal variability for $^{17}\Delta_{diss}$ was greatest in the North Inshore region, with a range from 68 ± 6 per meg in October 2006 to 108 ± 12 per meg in July 2006; and least in the Offshore region, with a range from 24 ± 3 per meg during July 2006 to 43 ± 7 per meg during January 2007 (Table 1; Fig. 3). The mean annual spatially weighted mixed-layer $^{17}\Delta_{diss}$ for the entire CalCOFI grid was 53 ± 5 per meg (Table 1).

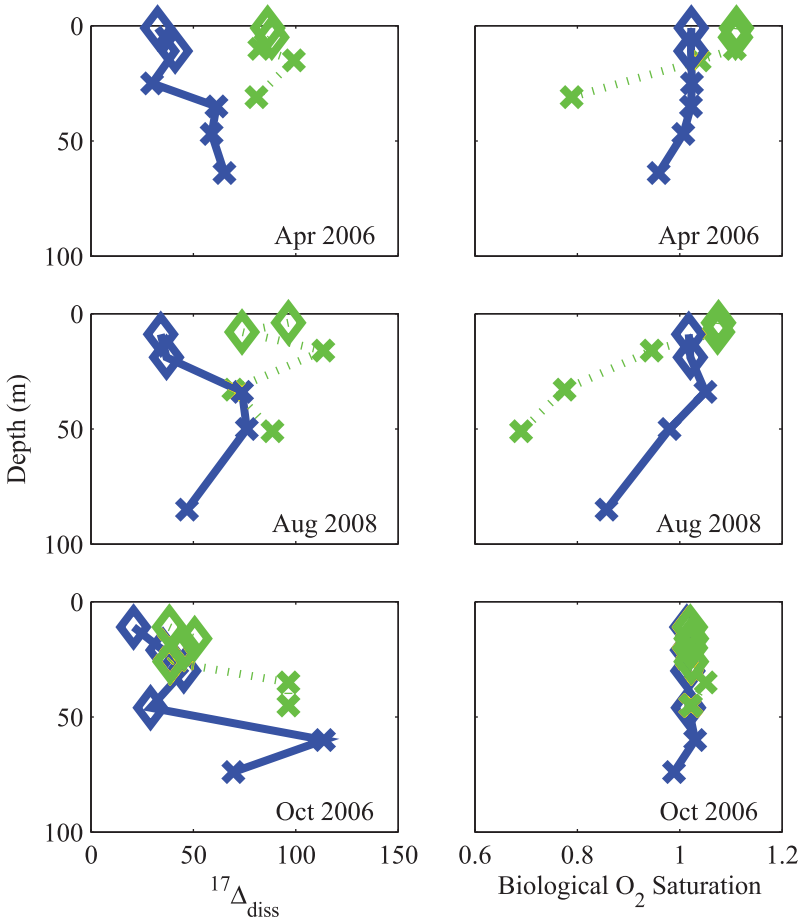

Fig. 2. Representative depth profiles of $^{17}\Delta_{diss}$ in parts per meg relative to air, and biological O_2 saturation $[(O_2:Ar)_{meas}/(O_2:Ar)_{sat}]$. Diamonds denote samples within the mixed layer. Xs denote samples beneath the mixed layer. Green lines indicate profiles located within the North and South Inshore regions; blue lines indicate profiles located within the California Current and Offshore regions.

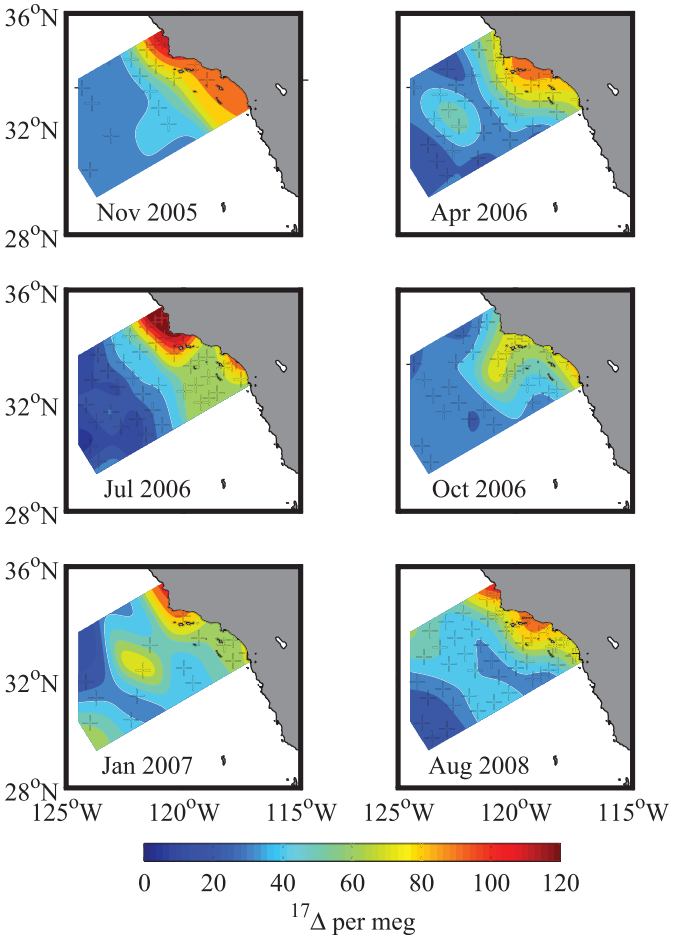

Fig. 3. Contour maps of mixed-layer $^{17}\Delta_{diss}$ in parts per meg for all six CalCOFI cruises. Plus symbols indicate stations where $^{17}\Delta_{diss}$ and O_2 : Ar samples were collected.

Mixed-layer $^{17}\Delta$-GOP rates were calculated using the approach outlined in Luz and Barkan (2011) and Prokopenko et al. (2011) with terms added for horizontal and vertical advection as in Eqs. 5 and 6; horizontal advection terms were neglected for the Offshore region because horizontal surface $^{17}\Delta_{diss}$ gradients were typically less than the uncertainty of mixed-layer $^{17}\Delta_{diss}$. $^{17}\Delta$-GOP rates were not calculated for the January 2007 cruise due to winter entrainment of high $^{17}\Delta_{diss}$ water beneath the mixed layer (mixed-layer depths during January 2007 were typically 2× those observed during the previous October). $^{17}\Delta$-GOP rates were also not calculated for the South Inshore region for the November 2005 cruise because mixed-layer samples were taken at only one station within the region and for the August 2008 cruise because the mixed-layer fraction of productivity based on ^{14}C-PP was $< 40\%$, indicating that $^{17}\Delta$-GOP mixed-layer budgets missed the majority of depth-integrated production. Annual mean mixed-layer productivity was greatest in the North Inshore region (326 ± 120 mmol O_2 m^{-2} d^{-1}) and least in the Offshore region (83 ± 39 mmol O_2 m^{-2} d^{-1}; Table 2). Temporal variability in $^{17}\Delta$-GOP was greatest in the North Inshore region, with a range from 234 ± 85 mmol O_2 m^{-2} d^{-1} to 533 ± 185 mmol O_2 m^{-2} d^{-1}; and least in the Offshore region, with a range from 49 ± 23 mmol O_2 m^{-2} d^{-1} to 121 ± 40 mmol O_2 m^{-2} d^{-1} (Table 3).

The effect of advection on $^{17}\Delta$-GOP estimates varied markedly from inshore regions moving offshore. The most significant corrections were applied to the California Current region, where the July 2006 $^{17}\Delta$-GOP values were reduced by 36%, from 98 mmol O_2 m^{-2} d^{-1} using the unapproximated version of Eq. 2 to 62 mmol O_2 m^{-2} d^{-1} including all advection terms (i.e., as in Eqs. 5 and 6). This was a result of high $^{17}\Delta_{diss}$ water from nearshore regions being advected offshore via Ekman transport. Advection corrections reduced mean annual $^{17}\Delta$-GOP rates by 12% in the California Current region and by negligible amounts for the North and South Inshore and Offshore regions. Advection reduced uncorrected mean annual $^{17}\Delta$-GOP estimates for the entire CalCOFI grid by 4% from 156 mmol O_2 m^{-2} d^{-1} to 151 mmol O_2 m^{-2} d^{-1}.

O_2 : Ar-NOP estimates—Mean mixed-layer biological O_2 saturation based on measured O_2 : Ar ranged from 1.008 ± 0.001 to 1.127 ± 0.024 for the four regions where uncertainties represent one SEM for each region (Table 1). Depth profiles show small biological O_2 saturation maxima associated with subsurface chlorophyll maxima and a consistent decrease with depth below the photic zone (Fig. 2). Annual mean biological O_2 saturation was highest in the North Inshore region (1.069 ± 0.012) and lowest in the Offshore region (1.013 ± 0.002; Table 1; Fig. 4). Seasonal variability was greatest in the North Inshore region, with a range from 1.037 ± 0.005 during October 2006 to 1.127 ± 0.024 during July 2006; and least in the Offshore region, with a range from 1.008 ± 0.001 in January 2007 to 1.017 ± 0.001 in October 2006 (Table 1; Fig. 4). Notably, biological O_2 saturation exceeded 1.000 for 297 of 310 (96%) individual mixed-layer samples. The mean annual biological O_2 saturation for the CalCOFI grid was 1.028 ± 0.005 (Table 1).

Mixed-layer O_2 : Ar-NOP was calculated using Eq. 7, which accounted for horizontal advection terms. Advection terms were negligible for the Offshore region. Annual O_2 : Ar-NOP was greatest in the North Inshore region (65 ± 18 mmol of O_2 m^{-2} d^{-1}) and least in the Offshore region (13 ± 4 mmol O_2 m^{-2} d^{-1}; Table 2). Temporal variability in O_2 : Ar-NOP was greatest in the North Inshore region, with a range from 18 ± 9 to 135 ± 31 mmol O_2 m^{-2} d^{-1}; and least in the Offshore region, with a range from 10 ± 3 to 16 ± 4 mmol O_2 m^{-2} d^{-1} (Table 3).

The effect of advection on O_2 : Ar-NOP estimates was greatest for the two inshore regions, with up to a 2× increase from 4 mmol O_2 m^{-2} d^{-1} to 8 mmol O_2 m^{-2} d^{-1} for the South Inshore region in January 2007 due to upwelling of water with significant biological undersaturation. Advection increased mean annual O_2 : Ar-NOP estimates by 44% and 57% in the North and South Inshore regions, respectively, and reduced rates by 6% and 3% in the California Current and Offshore regions, respectively. Advection increased the mean annual O_2 : Ar-NOP estimate for the CalCOFI grid by 21% from 20 mmol O_2 m^{-2} d^{-1} to 25 mmol O_2 m^{-2} d^{-1}.

Table 2. Annual production rates and ratios based on $^{17}\Delta_{diss}$, O_2 : Ar, ^{14}C incubations, and satellite observations. GOP—gross oxygen production; PP—primary production; NOP—net oxygen production; NCP—net carbon production; VGPM—Vertically Generalized Productivity Model; CbPM—Carbon based Productivity Model; HOTS—Hawaii Ocean Time-Series; BATS—Bermuda Atlantic Time-Series; nc—not calculated.

	Mixed-layer $^{17}\Delta$-GOP (mmol O_2 m^{-2} d^{-1})	Photic-zone $^{17}\Delta$-GOP (mmol O_2 m^{-2} d^{-1})	^{14}C-PP_{24h}* (mgC$m^{-2}d^{-1}$)	O_2 : Ar-NOP (mmol O_2 m^{-2} d^{-1})	O_2 : Ar-NCP† (mg C m^{-2} d^{-1})	VGPM-PP‡ (mg C m^{-2} d^{-1})	$VGPM_{cal}$-PP§ (mg C m^{-2} d^{-1})	CbPM-PP‖ (mg C m^{-2} d^{-1})	Mixed-layer $^{17}\Delta$-GOP : ^{14}C-PP_{24h}	Photic-zone $^{17}\Delta$-GOP : VGPM-PP	Mixed-layer O_2 : Ar-NOP : $^{17}\Delta$-GOP
Region 1: North Inshore	326±120	439±162	969±195	65±18	560±157	1738±356	1116±228	1029±184	5.9±0.8	3.4±0.6	0.20±0.06
Region 2: South Inshore	183±54	353±100	775±139	30±8	256±71	1017±128	653±82	790±128	5.4±1.0	3.9±0.5	0.16±0.06
Region 3: California Current	116±55	182±81	430±60	17±6	143±50	665±64	427±41	567±82	4.3±0.8	3.1±0.6	0.14±0.07
Region 4: Offshore	83±39	122±53	235±40	13±4	109±33	416±21	267±14	405±44	6.0±0.9	4.2±0.5	0.15±0.06
CalCOFI grid:	151±59	235±88	529±90	25±8	210±64	820±113	527±73	638±96	5.7±0.3	3.6±0.1	0.16±0.06
Other studies:											
HOT‖	nc	105±41	387±64	14±4	170±40	280±35	nc	nc	2.6–3.4	4.5	0.2±0.1
BATS¶ Seasonal range (May–Oct)	29–103	150–192	288–516	6–8	137–206	nc	nc	nc	4.4–9.9	nc	0.08–0.21

* CalCOFI ^{14}C-PP is converted from a 6 h to 24 h rate using the Eppley (1992) scaling factor of 1.81; HOT ^{14}C-PP is converted from a 12 h to 24 h rate assuming $^{14}C\text{-}PP_{24h} = 0.85 \times {}^{14}C\text{-}PP_{12h}$ (Karl et al. 1996).

† NOP is converted to NCP using a photosynthetic quotient of 1.4 (Laws 1991).

‡ Satellite-based estimates, VGPM-PP (Behrenfeld and Falkowski 1997) and CbPM-PP (Westberry et al. 2008), were obtained from the Ocean Productivity Group (Oregon State University).

§ $VGPM_{cal}$-PP is an empirically derived algorithm based on comparisons between CalCOFI ^{14}C-PP and VGPM-PP : $VGPM_{cal}\text{-}PP = 10^{\log(VGPM) - 0.1924}$ (Kahru et al. 2009).

‖ Estimates from Quay et al. (2010) and P. Quay (unpubl. data).

¶ Estimates from Luz and Barkan (2009); ^{14}C-PP converted from a 12 h to 24 h rate using the formula determined for HOT by Karl et al. (1996).

Table 3. Seasonal variability in production rates and ratios based on $^{17}\Delta_{diss}$, O_2 : Ar, ^{14}C incubations, and satellite observations. GOP—gross oxygen production; NOP—net oxygen production; PP—primary production; VGPM—Vertically Generalized Productivity Model; nc—not calculated.

	Mixed-layer $^{17}\Delta$-GOP (mmol O_2 m^{-2} d^{-1})	Photic-zone $^{17}\Delta$-GOP (mmol O_2 m^{-2} d^{-1})	O_2 : Ar-NOP (mmol O_2 m^{-2} d^{-1})	Mixed-layer $^{17}\Delta$-GOP : ^{14}C-PP_{24h}	Photic-zone $^{17}\Delta$-GOP : VGPM-PP	O_2 : Ar-NOP : $^{17}\Delta$-GOP
Region 1: North Inshore						
0511NH(Nov 2005)	399±137	nc	60±21	nc	nc	0.15±0.07
0604NH (Apr 2006)	309±100	415±135	88±20	5	2.2	0.29±0.05
0607NH (Jul 2006)	533±185	958±332	135±31	8.1	4.8	0.25±0.05
0610RR (Oct 2006)	234±85	334±121	38±15	6.8	3.6	0.16±0.12
0701JD (Jan 2007)	nc	nc	18±9	nc	nc	nc
0808NH (Aug 2008)	391±115	468±138	78±20	4.8	2.9	0.20±0.05
Region 2: South Inshore						
0511NH(Nov 2005)	nc	nc	nc	nc	nc	nc
0604NH (Apr 2006)	197±60	365±111	55±11	4.5	3.1	0.28±0.06
0607NH (Jul 2006)	188±56	466±138	50±11	8.1	4.3	0.26±0.10
0610RR (Oct 2006)	132±42	301±96	17±6	6.6	5.2	0.13±0.05
0701JD (Jan 2007)	nc	nc	8±6	nc	nc	nc
0808NH (Aug 2008)	nc	nc	27±7	nc	nc	nc
Region 3: California Current						
0511NH(Nov 2005)	133±52	160±63	11±5	3.4	2.8	0.08±0.03
0604NH (Apr 2006)	133±45	273±92	16±6	9.4	6.2	0.12±0.05
0607NH (Jul 2006)	62±40	146±93	20±8	3.3	2	0.33±0.23
0610RR (Oct 2006)	82±36	155±68	11±4	5.5	3.6	0.13±0.10
0701JD (Jan 2007)	nc	nc	17±6	nc	nc	nc
0808NH (Aug 2008)	134±50	196±73	26±7	4.8	3	0.19±0.05
Region 4: Offshore						
0511NH(Nov 2005)	121±40	160±52	10±4	6.9	4.9	0.08±0.03
0604NH (Apr 2006)	91±32	146±51	13±4	9.1	4.5	0.14±0.06
0607NH (Jul 2006)	49±23	71±33	12±3	3.1	2.3	0.23±0.20
0610RR (Oct 2006)	105±34	158±51	10±3	6.7	5.1	0.09±0.04
0701JD (Jan 2007)	nc	nc	14±4	nc	nc	nc
0808NH (Aug 2008)	78±29	164±60	16±4	5.7	4.2	0.21±0.09
CalCOFI Grid:						
0511NH(Nov 2005)	181±62	247±84	14±7	nc	3.6	0.08±0.04
0604NH (Apr 2006)	159±52	279±91	34±8	6.1	3.6	0.21±0.05
0607NH (Jul 2006)	150±58	307±118	40±10	5.9	3.5	0.26±0.17
0610RR (Oct 2006)	120±43	214±77	16±6	6.4	4.3	0.13±0.07
0701JD (Jan 2007)	nc	nc	14±6	nc	nc	nc
0808NH (Aug 2008)	144±49	246±86	30±8	5	3.4	0.21±0.06

NOP : GOP—NOP : GOP ratios for the mixed layer were calculated by dividing O_2 : Ar-NOP (Eq. 7) by $^{17}\Delta$-GOP (Eq. 5) for all cruises and regions except the January 2007 cruise due to the $^{17}\Delta_{diss}$ entrainment bias discussed above; estimates were also not calculated for the South Inshore region for November 2005 and August 2008 as discussed above. Annual means for NOP : GOP for the four regions ranged from 0.14 ± 0.07 in the California Current region to 0.20 ± 0.06 in the North Inshore region (Table 2). Temporal variability was similar for all regions. The seasonal range was largest for the California Current region (from 0.08 ± 0.03 to 0.33 ± 0.23) and least for the North Inshore region (from 0.15 ± 0.07 to 0.29 ± 0.05; Table 3). The annual mean for the entire CalCOFI grid was 0.16 ± 0.06 (Table 2).

Error analysis—Uncertainty in $^{17}\Delta$-GOP, O_2 : Ar-NOP, and NOP : GOP was estimated using a Monte Carlo analysis similar to the approach described in Juranek and Quay (2005). A mean value and error (± 1 SD) was assigned to each term in Eqs. 6 and 7; a value for each term was randomly selected assuming a normal distribution; and $^{17}\Delta$-GOP, O_2 : Ar-NOP, or NOP : GOP was calculated. The random selection process and calculations were repeated 1000 times and the uncertainty was calculated as ± 1 SD for all 1000 values.

Assigned errors (± 1 SD) for the parameters in Eqs. 6 and 7 applied in the Monte Carlo analysis are as follows: 25% for K_g (i.e., the range in K_g for different gas exchange parameterizations); 0.2% for C_{sat}; 15 per meg for $^{17}\Delta_p$ and 2 per meg for $^{17}\Delta_{eq}$ (Luz and Barkan 2000); 4–7 per meg for $^{17}\Delta_{diss}$ (i.e., the SEM of all mixed-layer values within each region as given in Table 1); 10 per meg for $^{17}\Delta_z$ (i.e., the SD of the vertical gradient in $^{17}\Delta_{diss}$); 0.2–1.2% for $(O_2 : Ar)_{bio\_ml}$ (i.e., the SEM of all mixed-layer values within each region

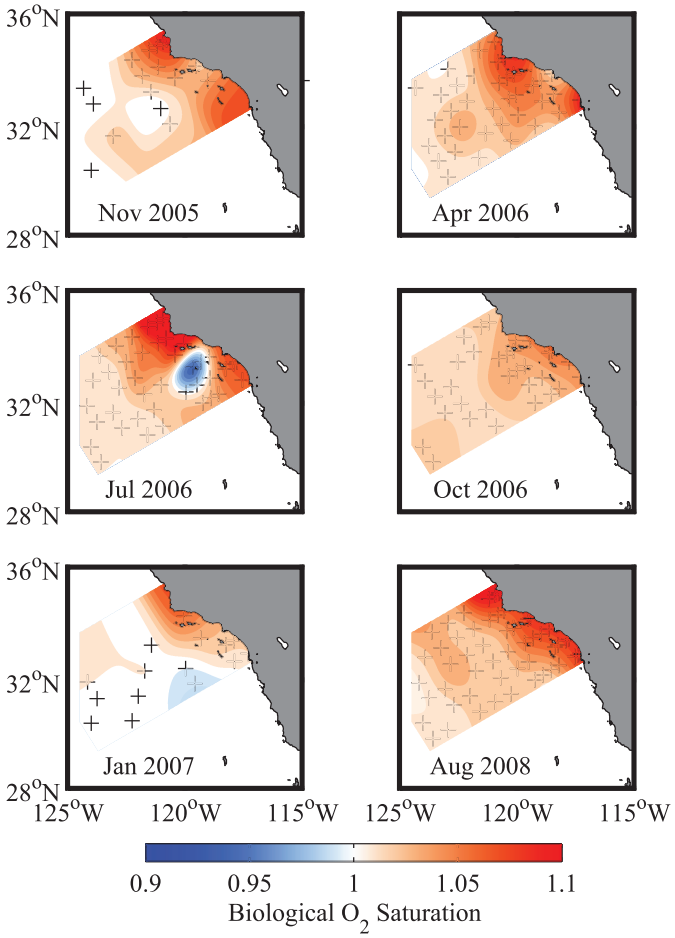

Fig. 4. Contour maps of mixed-layer biological O_2 saturation for all six CalCOFI cruises. Plus symbols indicate stations where $^{17}\Delta_{diss}$ and O_2 : Ar samples were collected.

as given in Table 1); 1.5% for $(O_2:Ar)_{bio\_z}$ (i.e., the SD of the vertical gradient in biological O_2 saturation); 7 mmol m^{-3} for C_{ml} (i.e., the typical SD of all mixed-layer estimates within each region); 7 cm s^{-1} for geostrophic current velocities and 0.2 cm s^{-1} for Ekman velocities (i.e., the typical SD of all velocity estimates across a given boundary); 0.5 m d^{-1} for w_{coast} in the two inshore regions (i.e., the SD of simultaneous w_{coast} estimates for two buoys within the North Inshore region); 0.02 m d^{-1} for w_{curl} in all regions (i.e., the typical SD of individual w_{curl} estimates within a given region). Note that the sensitivity of GOP to $^{17}\Delta_{diss}$ increases as $^{17}\Delta_{diss}$ approaches $^{17}\Delta_{eq}$, whereas the fractional uncertainty in K_g remains constant for all GOP and NOP estimates.

Time and space integration of different PP methods—Comparisons between different productivity methods are complicated by the different integration times of each method. The ^{14}C-PP method represents a snapshot of the period of hours over which incubation experiments are conducted (i.e., 6 h for ^{14}C-PP experiments conducted during CalCOFI cruises). The $^{17}\Delta$-GOP and O_2:Ar-NOP methods integrate over the residence time of O_2 in the mixed layer, which is typically 4–8 d in the CalCOFI region. To account for the different integration periods of the two methods, we average ^{14}C-PP both temporally and spatially as done for $^{17}\Delta$ and O_2:Ar measurements. The ^{14}C-PP calculated for each region (Fig. 1) and cruise represents the mean of three to five different ^{14}C-PP incubations conducted over 5–10 d, which is close to the residence time of O_2 in the mixed layer. We also determine the fraction of ^{14}C-PP occurring in the mixed layer relative to the photic zone for each station where incubations were conducted; the mean of the mixed-layer fraction of ^{14}C-PP for all stations within a given region is then used to extrapolate the mixed-layer $^{17}\Delta$-GOP rate to a photic zone rate. The satellite-based productivity estimates are also averaged temporally and spatially to provide a more meaningful comparison; VGPM and CbPM estimates represent 16 d composites on a 10 km spatial scale during which ship-based productivity measurements were conducted. The regional estimate for VGPM-PP and CbPM-PP represents the mean of all individual observations (typically several hundred) within each region.

Annual means for all productivity estimates (Table 2) were calculated by first averaging cruise estimates seasonally over 3 month intervals (i.e., January to March, April to June, July to September, and October to December). $^{17}\Delta$-GOP for each region during the January to March interval was estimated using the regional mean $^{17}\Delta$-GOP : ^{14}C-PP slope for the five other cruises (i.e., cruises that took place in spring, summer, and autumn) and measured ^{14}C-PP. Annual means presented in Table 2 for ^{14}C-PP, VGPM-PP, and CbPM-PP are within 15% of long-term annual means calculated for the period from 2000 to 2009 for all regions except the North Inshore region, where the annual ^{14}C-PP was ~ 30% lower than the long-term annual mean. The low annual ^{14}C-PP for the North Inshore region may be due to undersampling of high-productivity stations in the North Inshore region during cruises also sampled for $^{17}\Delta$ and O_2:Ar because the annual VGPM-PP estimate for this region (Table 2) was 10% above the long-term mean. The $^{17}\Delta$-GOP : ^{14}C-PP relationship determined on a station by station basis for all stations not influenced by significant advection transports is nearly the same as the relationship determined using the seasonal and regional averaging scheme described above (i.e., the $^{17}\Delta$-GOP : ^{14}C-PP slope for the station by station analysis was 5.4 compared with the slope of 5.6 presented in Fig. 5).

Discussion

Spatial and seasonal trends in $^{17}\Delta$-GOP, ^{14}C-PP, and satellite-based PP—The spatial and seasonal range in photic zone $^{17}\Delta$-GOP for all four regions reported here (71–958 mmol O_2 m^{-2} d^{-1}) is similar to the range in $^{17}\Delta$-GOP reported by Sarma et al. (2008) for Sagami Bay off the coast of Japan in May 2006 (34–963 mmol O_2 m^{-2} d^{-1}), which is the only other location where $^{17}\Delta$-GOP rates have been reported for the coastal ocean. Annual photic zone $^{17}\Delta$-GOP for the entire CalCOFI region (235 ± 88 mmol O_2 m^{-2} d^{-1}) is more than 2.2× mean annual $^{17}\Delta$-GOP in the subtropical North Pacific at HOT (105 ± 41 mmol O_2

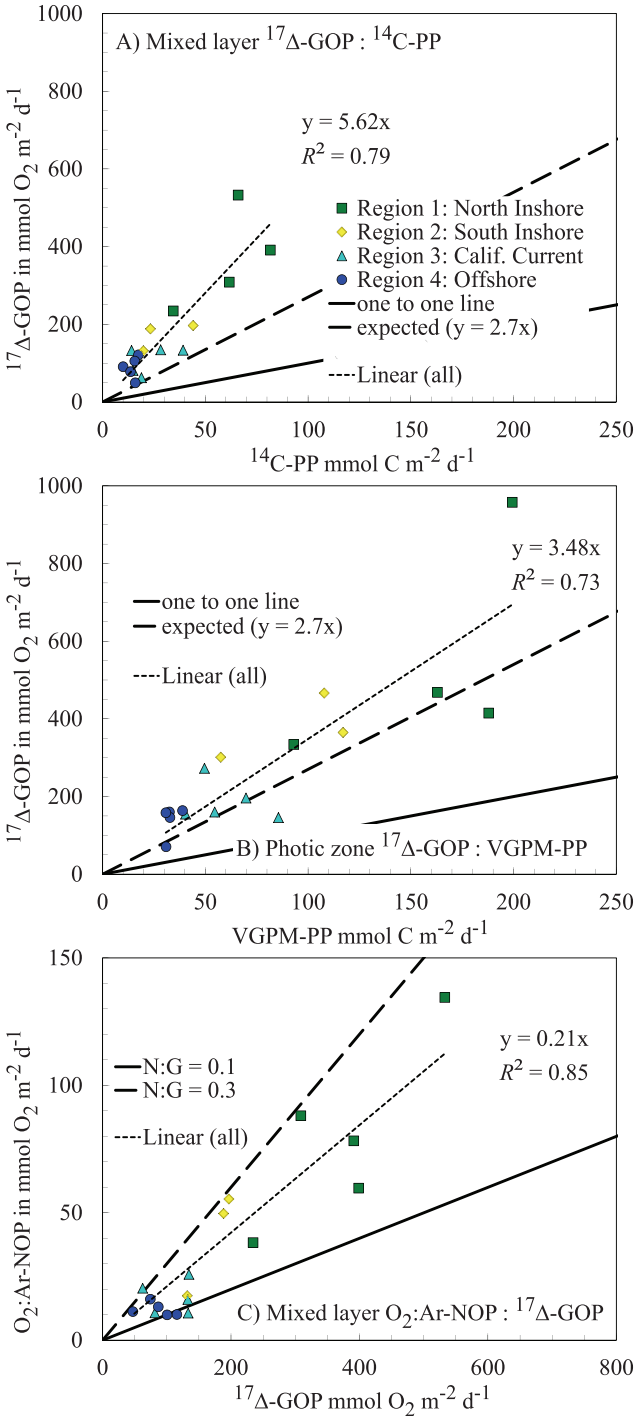

Fig. 5. The relationship between (A) mixed-layer $^{17}\Delta$-GOP and mixed-layer ^{14}C-PP$_{24h}$; (B) photic zone $^{17}\Delta$-GOP and photic zone VGPM-PP; and (C) mixed-layer O_2 : Ar-NOP and mixed-layer $^{17}\Delta$-GOP for all cruises except 0701JD. Productivity calculations were not made for the January cruise 0701JD due to the entrainment bias discussed in the text. N : G—the ratio of net O_2 production to gross O_2 production.

m^{-2} d^{-1}; Quay et al. 2010) and 1.2× the highest $^{17}\Delta$-GOP reported from May to October of 2000 in the subtropical North Atlantic at BATS (150–192 mmol O_2 m^{-2} d^{-1}; Luz and Barkan 2009). Annual mean $^{17}\Delta$-GOP for the Offshore region at CalCOFI (122 ± 53 mmol O_2 m^{-2} d^{-1}) is comparable to rates observed in the oligotrophic ocean at HOT and BATS (Table 2).

Spatially, annual $^{17}\Delta$-GOP and ^{14}C-PP$_{24h}$ exhibited similar variability between regions; annual $^{17}\Delta$-GOP and ^{14}C-PP$_{24h}$ for the North Inshore region were 3.9× and 4.1×, respectively, annual rates in the Offshore region (Table 2). Spatial variability of VGPM-PP was similar to that of $^{17}\Delta$-GOP, while CbPM-PP was less variable between regions (Table 2). Annual mean VGPM-PP and CbPM-PP for the North Inshore region were 4.2× and 2.5× rates in the Offshore region, respectively (Table 2). Seasonal variability for all methods was largest in the North Inshore region (Table 3); summer photic-zone $^{17}\Delta$-GOP was 2.9× rates observed during autumn (winter $^{17}\Delta$-GOP rates are not reported due to the entrainment bias). The Offshore region was least variable from cruise to cruise for all PP methods except $^{17}\Delta$-GOP, which was least variable in the South Inshore region (Table 3). The uncertainty in $^{17}\Delta$-GOP estimates makes the seasonal range difficult to distinguish in oligotrophic regions of the North Pacific as noted by Quay et al. (2010).

Comparisons of $^{17}\Delta$-GOP with ^{14}C-PP—Annual mean $^{17}\Delta$-GOP (mmol O_2 m^{-2} d^{-1}) estimated for each region was 4–6× bottle ^{14}C-PP$_{24h}$ (mmol C m^{-2} d^{-1}; Table 2; Fig. 5). The mixed-layer $^{17}\Delta$-GOP : ^{14}C-PP$_{24h}$ was more variable on a seasonal basis (Table 3), with ratios > 9 observed in spring (April 2006) for the California Current and Offshore regions and in summer (July 2006) for the inshore regions; the lowest ratio (near 3.1) was observed in the Offshore region during July 2006 (Table 3). The seasonal range of $^{17}\Delta$-GOP : ^{14}C-PP$_{24h}$ for the CalCOFI grid of 3.1–9.4 (Table 3) is similar to the range observed at BATS (4.4–9.9) by Luz and Barkan (2009) but significantly higher than the range observed at HOT (2.6–3.4) by Quay et al. (2010; Table 2). It should be noted that some of the variability in the $^{17}\Delta$-GOP : ^{14}C-PP results from the conversion of shorter duration ^{14}C-PP incubation experiments at CalCOFI (6 h), BATS (12 h), and HOT (12 h) to 24 h rates as described above and from the uncertainty in $^{17}\Delta$-GOP (± 30%; Table 2). We explore several possible explanations for the variation in $^{17}\Delta$-GOP : ^{14}C-PP$_{24h}$ ratios observed at CalCOFI, HOT, and BATS: (1) variability in the O_2 production : carbon fixation ratio, (2) entrainment of high $^{17}\Delta$ water from the deep photic zone into the mixed layer, and (3) ^{14}C-PP methodological effects.

In a study of Lake Kinneret, Luz et al. (2002), observed ^{18}O-GOP : ^{14}C-PP ratios of 1.9 for nonbloom conditions and 7.5 for bloom conditions, comparable to the seasonal range observed during our study (3.1–9.4). Robinson et al. (2009) observed ^{18}O-GOP : ^{14}C-PP ratios > 5 at a diatom-dominated station in the Celtic Sea. One possible explanation for these high ^{18}O-GOP : ^{14}C-PP ratios is that the O_2 production to carbon fixation ratio increases under high light conditions, as discussed in Zehr and Kudela (2009). Although variability in light conditions may contribute to the high seasonal variability in $^{17}\Delta$-GOP : ^{14}C-PP$_{24h}$ ratios at CalCOFI and BATS relative to HOT, it does not seem likely that variability in light conditions can explain the

disparity between the annual mean $^{17}\Delta$-GOP : ^{14}C-PP$_{24h}$ ratio of $\sim$ 3 at HOT (Quay et al. 2010) and $\sim$ 6 for the Offshore region at CalCOFI, given that both sites are located in the oligotrophic subtropical North Pacific (Table 2). In any case, a better understanding of the variability in rates of photosynthetic O_2 production and corresponding carbon fixation for different plankton species under different light and nutrient conditions is clearly needed.

Entrainment of high $^{17}\Delta$ water beneath the mixed layer (Fig. 2) can inflate $^{17}\Delta$-GOP rates, which could also lead to higher than expected $^{17}\Delta$-GOP : ^{14}C-PP$_{24h}$ ratios. Nicholson et al. (2012) demonstrated using a one-dimensional model that high mixed-layer ratios observed at BATS (Luz and Barkan 2009) were likely due to entrainment of high $^{17}\Delta$ water from the deep photic zone. We note that $^{17}\Delta$ depth profiles at CalCOFI typically display smaller subsurface maxima than at BATS, where a large fraction of the photic zone is beneath the mixed layer during the summer and autumn. At CalCOFI, the South Inshore region, which includes the sheltered Southern California Bight, develops strong subsurface maxima in $^{17}\Delta$ in the late summer and early autumn, which could lead to significant entrainment bias. We have excluded $^{17}\Delta$-GOP estimates for this region for the August 2008 cruise where $< 40\%$ of ^{14}C-PP occurred within the mixed layer because mixed-layer budgets missed a large fraction of the total photic zone production and because of the potential for entrainment bias (Table 3). In contrast, vertical profiles in high-productivity inshore regions show no identifiable maximum in the deep photic zone, which suggests entrainment bias in these regions is negligible (Fig. 2). Although we cannot rule out the potential for entrainment bias in other regions, we note that on average annual $^{17}\Delta$-GOP : ^{14}C-PP$_{24h}$ ratios are consistent for all four regions (Table 2) and that during the most productive times of year, the bulk of ^{14}C-PP ($> 80\%$) occurs in the mixed layer, which (combined with high vertical velocities due to coastal and curl-driven upwelling) limits the development of large sub–mixed-layer $^{17}\Delta$ maxima characteristic of more stratified oligotrophic regions.

Another possible explanation for high $^{17}\Delta$-GOP : ^{14}C-PP$_{24h}$ rates observed during CalCOFI cruises is that ^{14}C-PP increasingly underestimates PP at high productivity rates. Effects that could be responsible for ^{14}C-PP underestimation include high rates of DO^{14}C excretion, heterotrophic recycling of ^{14}C during incubations, and internal recycling of unlabeled CO_2 (Marra 2002). Karl et al. (1998) measured DO^{14}C excretion rates at HOT that accounted for up to 30% of PO^{14}C uptake. Additionally, the importance of heterotrophic recycling of PO^{14}C and internal recycling of unlabeled CO_2 could increase as the PP rate increases, yielding greater underestimates of PO^{14}C production at high rates of PP. Given that annual $^{17}\Delta$-GOP : ^{14}C-PP$_{24h}$ ratios were similar in the lower productivity Offshore region (6.0 ± 0.9) and the high-productivity North Inshore region (5.9 ± 0.8) and that the $^{17}\Delta$-GOP : ^{14}C-PP$_{24h}$ ratio itself did not increase at greater ^{14}C-PP rates (Fig. 5), it does not seem likely that effects related to increasing PP rates can account for differences in $^{17}\Delta$-GOP : ^{14}C-PP$_{24h}$ ratios between HOT and CalCOFI. High rates of DO^{14}C excretion, on the other hand, could contribute to consistently higher $^{17}\Delta$-GOP : ^{14}C-PP$_{24h}$ ratios at CalCOFI. Although rates of DO^{14}C excretion were not determined on CalCOFI cruises, if we assume that DO^{14}C accounted for 30% of PO^{14}C uptake at CalCOFI, the annual $^{17}\Delta$-GOP : ^{14}C-PP$_{24h}$ ratio for the Offshore region is reduced from 6.0 ± 0.9 to 4.2 ± 0.6, which is still outside the range of ratios observed at HOT (2.6–3.4; Table 2) and significantly different from the annual mean $^{17}\Delta$-GOP : ^{14}C-PP$_{24h}$ ratio at the 95% confidence level.

Another methodological issue that could contribute to differences between the long-term mean ^{14}C-PP$_{24h}$ at HOT (400 mg C m^{-2} d^{-1}; Karl et al. 1998) and the annual mean for the CalCOFI Offshore region (235 ± 40 mg C m^{-2} d^{-1}) may be systematic differences between on-deck simulated in situ (SIS) and in situ (IS) bottle incubation (in contrast, $^{17}\Delta$-GOP estimates for the two studies were based on $^{17}\Delta$ measurements made by the same research group using similar calculation procedures). The ^{14}C-PP method at HOT utilizes in situ bottle incubation at five depths from 5 m to 125 m between dawn and dusk, whereas the CalCOFI ^{14}C-PP method utilizes on-deck incubation for 6 h where on-deck incubators are temperature-regulated with surface seawater and in situ light conditions simulated using neutral density screens. Grande et al. (1989) observed greater ^{18}O-GOP$_{SIS}$: ^{14}C-PP$_{SIS}$ (on-deck) ratios (2.2) relative to ^{18}O-GOP$_{IS}$: ^{14}C-PP$_{IS}$ (in situ) ratios (1.4), which they attributed to differences in the spectral composition of light filtered through neutral density screens compared with light in situ. Other studies observed suppression of ^{14}C assimilation using on-deck incubators, possibly due to photoinhibition (Marra 1980). If we assume that on-deck methodology contributed to underestimation of ^{14}C-PP$_{24h}$ by 35%, as suggested by Grande et al. (1989), the annual $^{17}\Delta$-GOP : ^{14}C-PP$_{24h}$ ratio for the Offshore region is reduced from 6.0 to 4.4. Recent ^{14}C-PP estimates for the CalCOFI region using the same 24 h in situ methodology employed at HOT also suggest that on-deck incubations underestimate ^{14}C-PP. Stukel et al. (2011) measured ^{14}C-PP within the Offshore region (i.e., Region 4 of this study) of 520 mg C m^{-2} d^{-1} during a California Current Ecosytem Long Term Ecological Research cruise in May and June 2006; the ^{14}C-PP estimate for the Offshore region during the April 2006 CalCOFI cruise was 200 mg C m^{-2} d^{-1} (where the CalCOFI ^{14}C-PP has been scaled to a 24 h rate using the factor of 1.81 discussed above). We also note that recent comparisons of mixed-layer $^{17}\Delta$-GOP and ^{14}C-PP off the central California coast (D. Munro unpubl.) yielded $^{17}\Delta$-GOP : ^{14}C-PP ratios between two and three, which agrees with comparisons of incubation-based ^{18}O-GOP and ^{14}C-PP (Marra 2002) and also suggests methodological biases in ^{14}C-PP at CalCOFI. It is possible that the combined effects of DO^{14}C excretion and on-deck incubation could account for the 2$\times$ higher $^{17}\Delta$-GOP : ^{14}C-PP$_{24h}$ ratios observed at CalCOFI compared with HOT.

Comparisons of $^{17}\Delta$-GOP and ^{14}C-PP with satellite PP—The mean ^{14}C-PP$_{24h}$: VGPM-PP and ^{14}C-PP$_{24h}$: CbPM-PP ratios (PP estimates in mg C m^{-2} d^{-1}) for all stations and

cruises were 0.62 ± 0.03 and 0.90 ± 0.07, respectively. The ^{14}C-PP$_{24h}$: VGPM-PP relationship is consistent with previous results for the CalCOFI region and has been assumed to indicate an overestimation of PP by the VGPM in the coastal ocean (Kahru et al. 2009). More recent productivity models, including the CbPM estimate, significantly lower PP for high-productivity regions such as the North Inshore region in this study (Table 2). Kahru et al. (2009) presented an empirically derived modification of the VGPM algorithm (VGPM$_{cal}$) based on comparisons with CalCOFI ^{14}C-PP, which reduces VGPM-PP estimates by 36% (Table 2). At HOT, ^{14}C-PP$_{24h}$: VGPM-PP ratio was 1.38 (P. Quay unpubl.), where ^{14}C-PP$_{12h}$ was converted to ^{14}C-PP$_{24h}$ as described above and in Table 2. That the ^{14}C-PP$_{24h}$: VGPM of 0.6 in the Offshore region of CalCOFI is only half that observed at HOT is surprising and may be related to the ^{14}C-PP methodological issues at CalCOFI discussed above rather than overestimation of PP by the VGPM.

At CalCOFI, the $^{17}\Delta$-GOP : VGPM-PP and $^{17}\Delta$-GOP : CbPM-PP ratios using the photic zone GOP estimates described above were 3.5 ± 0.3 and 4.8 ± 0.5, which are close to previous estimates using the $^{17}\Delta$ method. At HOT, the $^{17}\Delta$-GOP : VGPM-PP ratio was 4.5 (P. Quay unpubl.). For further comparison, Juranek and Quay (2010) report $^{17}\Delta$-GOP : VGPM-PP and $^{17}\Delta$-GOP : CbPM-PP ratios for the equatorial Pacific of 7.0 and 4.6, respectively, and Reuer et al. (2007) observed a $^{17}\Delta$-GOP : VGPM-PP of 5.4 in the Southern Ocean. The disparity between $^{17}\Delta$-GOP, ^{14}C-PP, and satellite PP for different regions highlights the substantial uncertainty of each PP method and emphasizes the need to utilize multiple approaches whenever possible.

Net carbon production (NCP) and NOP : GOP—The annual rate of NCP (equivalent to organic carbon export at steady state) estimated from O_2 : Ar ranged from 109 mg C m^{-2} d^{-1} (3.3 mol C m^{-2} yr^{-1}) for the Offshore region to 560 mg C m^{-2} d^{-1} (17.0 mol C m^{-2} yr^{-1}) for the North Inshore region; the spatially weighted annual rate for the entire CalCOFI grid was 210 mg C m^{-2} d^{-1} (6.4 mol C m^{-2} yr^{-1}). The conversion from O_2 to carbon units assumed a photosynthetic quotient of 1.4 as described above. Previous NCP estimates for different regions within the CalCOFI grid are presented in Table 4. Our O_2 : Ar-NCP estimates agree closely with new production estimates based on f-ratios from ^{15}N uptake experiments and ^{14}C-PP$_{24h}$ in the CalCOFI region (204 mg C m^{-2} d^{-1}; Dugdale and Wilkerson 1992; Eppley 1992), and are more than 2× greater than POC flux estimates based on sediment trap (Collins et al. 2011) and ^{234}Th (Stukel et al. 2011) measurements within the North and South Inshore regions (Table 4). That POC export estimates are significantly lower than O_2 : Ar-NCP is expected due to potentially large differences in the spatial integration scale of these measurements and the contribution of the DOC component of the export flux, as observed at HOT by Emerson et al. (1997).

NOP : GOP ratios determined by measurements of $^{17}\Delta_{diss}$ and O_2 : Ar during CalCOFI ranged from 0.08 ± 0.03 to 0.33 ± 0.23 (Table 3). NOP : GOP increased only slightly with increasing productivity (Fig. 5). For comparison, the range in NOP : GOP based on O_2 : Ar and $^{17}\Delta_{diss}$ measurements reported by Sarma et al. (2008) for Sagami Bay off Japan was −0.49 to 0.28 where the negative values were confined to a small spatial region near the outflow of the Sakawa River. Estimated NOP : GOP at CalCOFI is strikingly similar to estimates at open-ocean sites where contemporaneous O_2 : Ar and $^{17}\Delta_{diss}$ measurements have been made. At HOT, Quay et al. (2010) reported a winter mean of 0.13 ± 0.05 and summer mean of 0.22 ± 0.06, similar to the range reported by Luz and Barkan (2009) at BATS (0.08–0.21). For further comparison, Stanley et al. (2010) reported a mean NOP : GOP ratio of 0.06 ± 0.02 in the equatorial Pacific; and Reuer et al. (2007) reported a mean of 0.13 in the Southern Ocean.

Previous estimates of organic carbon export efficiency in the CalCOFI region have been based on an f-ratio determined from incubation measurements. For example, Eppley et al. (1979) and Eppley (1992) reported f-ratios based on $^{15}NO_3$-uptake-based estimates of NCP and ^{14}C-PP of 0.36 and 0.33 for the Southern California Bight (comparable to the South Inshore region), respectively. Dugdale and Wilkerson (1992) reported an f-ratio based on $^{15}NO_3$ and $^{15}NH_4$ uptake of 0.57 in the upwelling region near Point Conception, with values > 0.8 during the height of bloom conditions. We estimated an equivalent f-ratio by converting NOP to NCP (as described above) and dividing by ^{14}C-PP$_{24h}$. This calculation yielded a mean annual f-ratio (in carbon units) for the CalCOFI grid, North Inshore, South Inshore, California Current, and Offshore regions of 0.40, 0.58, 0.33, 0.33, and 0.46, respectively. Alternately, f-ratios were calculated by converting our NOP : GOP ratio to NCP : ^{14}C-PP$_{24h}$, where O_2 : Ar-NOP was divided by 1.4 to yield NCP and $^{17}\Delta$-GOP was divided by 2.7 (Marra 2002) to yield ^{14}C-PP, as described above. This calculation yields mean annual f-ratios for the CalCOFI grid, North Inshore, South Inshore, California Current, and Offshore regions of 0.32, 0.39, 0.31, 0.28, and 0.29, respectively. Differences may result from variability in the relationship between O_2 production and carbon fixation and/or underestimation of ^{14}C uptake by on-board incubation methods as discussed above. It is important to recognize that the NOP : GOP ratio determined from O_2 : Ar and $^{17}\Delta_{diss}$ represents a new gauge of potential export efficiency that should not necessarily be expected to agree with incubation-based approaches. In any case, NOP : GOP estimates based on O_2 : Ar and $^{17}\Delta_{diss}$ suggest potential export efficiency (~ 0.15) throughout the CalCOFI region remarkably close to efficiencies of open-ocean environments determined using the same method (Table 2).

Export production in the California Current Ecosystem—Several studies based on both in situ (Thunell 1998; Stukel et al. 2011) and modeling (Olivieri and Chavez 2000) approaches suggest that POC export may be inversely related to PP in the California Current Ecosystem. These studies also suggest that much of the organic material fixed in high-productivity regions inshore of the California Current may be advected offshore in the Ekman layer.

Table 4. Comparison of export production estimates from different studies in the California Current System.

Authors	Method	Region	Estimated carbon export (mg C m^{-2} yr^{-1})	Estimated carbon export (mol C m^{-2} yr^{-1})
This study	O_2 : Ar-NCP mixed layer	North Inshore	560	17.0
		South Inshore	256	7.8
		California Current	143	4.3
		Offshore	109	3.3
		CalCOFI grid	210	6.4
Dugdale and Wilkerson 1992; Eppley 1992	^{15}N uptake-based f-ratio × ^{14}C-PP* photic zone	North Inshore	553	16.8
		South Inshore	256	7.8
		California Current	142	4.3
		Offshore	77	2.3
		CalCOFI grid	205	6.2
Collins et al. 2011	sediment trap 100 m	San Pedro Basin	134	4.1
Stukel et al. 2011	^{234}Th POC export†	North Inshore	123	3.7
		California Current	72	2.2
		Offshore	76	2.3
Roemmich 1989	nutrient budget	CalCOFI grid	240	7.3
Bograd et al. 2001	nutrient budget	CalCOFI grid	327	9.9
Messié et al. 2009	nutrient budget	North Inshore (32.9–35 N)	622	18.9
Pennington et al. 2010	nutrient budget	Coastal Upwelling Region off Monterey Bay (comparable to North Inshore)	559	17.0

* New production calculated from f-ratios based on ^{15}N uptake experiments for the Point Conception region (f = 0.57) reported by Dugdale and Wilkerson (1992) and for the Southern California Bight (f = 0.33) reported by Eppley (1992) multiplied by ^{14}C-PP from the six cruises where $^{17}\Delta_{diss}$ and O_2 : Ar were also measured.

† ^{234}Th particulate organic carbon (POC) export estimates were made for three regions within the Southern California Current System comparable to regions discussed in this study. Two measurements were made in the region inshore of the California Current (comparable to our North Inshore region); these estimates are averaged.

Our results of potential export efficiency based on the NOP : GOP ratio indicate lower efficiency in the productive North Inshore region compared with estimates of the f-ratio based on incubation experiments (Dugdale and Wilkerson 1992). Additionally, our results yield much higher estimates of NCP in the North Inshore region compared with past estimates of POC export (Table 4), indicating that a large fraction (up to 75%) of the organic material produced in the high-productivity regions inshore of the California Current does not sink out of the surface ocean within the inshore regions.

Comparison of our estimates with other budget estimates for the entire CalCOFI grid provides some indication about the fate of the organic material registered as NCP using the O_2 : Ar approach. Our mean O_2 : Ar-NCP estimate (210 mg C m^{-2} d^{-1}) for the CalCOFI grid is within the interannual variability of estimates determined for 1984–1987 by Roemmich (1989; annual mean of 240 mg C m^{-2} d^{-1}) and for 1984–1997 by Bograd et al. (2001; annual mean of 327 mg C m^{-2} d^{-1}), who both estimated NCP based on a nutrient (NO_3^- and PO_4^{3-}) budget (assuming Redfield stoichiometry of 106 : 16 : 1 in relating C : N : P) for a control volume (bounded by CalCOFI line 77 to the north, line 93 to the south, Sta. 100 to the west, and extending to a depth of 500 m) utilizing measured nutrient concentrations and geostrophic and Ekman transport estimates. The NCP estimates of Roemmich (1989) and Bograd et al. (2001) are potentially lower than NCP in the mixed layer because some of the exported NCP is remineralized within the control volume (which extends to 500 m). Agreement between our O_2 : Ar-NCP rates and the nutrient-budget-based estimates of Roemmich (1989) and Bograd et al. (2001) has three important implications: (1) that organic carbon export in the CalCOFI region is supported almost entirely by nutrients supplied from outside the control volume (i.e., nonlocal sources); (2) that respiration between the mixed layer and 500 m is low within the CalCOFI grid; and (3) that most of the NCP that occurs within the control volume is advected horizontally out of the control volume in the Ekman layer. This final conclusion is based on sediment-trap studies in the central CCS (Knauer and Martin 1981) that indicated low POC flux at 500 m and the assumption that POC export to the narrow shelf in this region accounted for a relatively small fraction of NCP for the entire CalCOFI grid. With regard to the suggestion that the respiration rate is low between the mixed layer and 500 m, the uncertainties in both methods complicate accurate estimation of the deep respiration rate. We note that the study of Bograd et al. (2001) indicates significant interannual variability in NCP, with annual rates from 1993 to 1997 more than 2.7× rates observed from 1988 to 1992. We believe that it is unlikely that the O_2 : Ar-NCP estimate is biased low given agreement between our estimate presented here and estimates of potential new production (an upper limit on export production) based on nitrate supply for the CalCOFI region (Messié et al. 2009) and carbon budgets for other upwelling regions of the CCS (Pennington et al. 2010; Table 4). We also note that our O_2 : Ar NCP estimates are within 10% of O_2-based NCP estimates from

a more extensive analysis of the CalCOFI data set (i.e., from 1984 to 2010; D. Munro unpubl.).

$^{17}\Delta$-GOP and O_2 : Ar-NOP productivity estimates in the California Current Ecosystem—We highlight the following five observations and implications of the productivity estimates presented here. (1) PP as determined by the $^{17}\Delta$-GOP, ^{14}C-PP, and VGPM methods increases by a factor of four from the subtropical North Pacific to regions inshore of the California Current. (2) The ratio of $^{17}\Delta$-GOP : ^{14}C-PP is twice that expected from previous comparisons of incubation experiments (i.e., ^{18}O-GOP : ^{14}C-PP), which may result from methodological issues with ^{14}C-PP measurement or biases in the $^{17}\Delta$-GOP method including variable ratios of O_2 : C production. (3) The photic-zone $^{17}\Delta$-GOP : VGPM-PP ratios of 4–5 are the same as those found at HOT using the same methods. Ratios of ^{14}C-PP : VGPM-PP of 0.6 in the CalCOFI region may be a result of methodological problems with ^{14}C-PP rather than overestimation by the VGPM. (4) The potential e-ratio in O_2 units (i.e., O_2 : Ar-NOP : $^{17}\Delta$-GOP) of 0.16 is surprisingly similar to measurements made in the subtropical North Pacific at HOT using the same methods, which implies efficiency of organic carbon production in coastal oceans similar to that in the open oligotrophic ocean. (5) O_2 : Ar-NCP estimates are much higher than sediment trap and ^{234}Th estimates of POC flux, which implies either methodological biases in approaches or that DOC is an important component of the export flux. Agreement between O_2 : Ar-NCP and nitrate budget estimates of NCP implies little respiration of 'exportable' organic carbon beneath the mixed layer within the coastal ocean. This result is consistent with a recent study by Deutsch et al. (2011) that suggests recent observations of lower O_2 concentrations at depth in the CalCOFI region (Bograd et al. 2008) may be a result of transport of low-O_2 waters into the CCS rather than an increase in respiration beneath the mixed layer. However, accurate estimation of the deep respiration rate is complicated by uncertainties in the mixed-layer NCP estimates presented here and NCP estimates integrating to 500 m (Bograd et al. 2001).

In summary, $^{17}\Delta$-GOP and O_2 : Ar-NOP nonincubation results provide a significantly different view of PP and NCP in the CalCOFI region compared with results based on incubation and satellite-based methods. Thus, the recommendation from this and similar recent studies (Juranek and Quay 2005; Robinson et al. 2009; Quay et al. 2010) is to adopt a multipronged approach to PP and NCP measurement utilizing a suite of methods, each with their own biases, that in combination should better constrain biological productivity rates in the coastal ocean.

Acknowledgments

We acknowledge all technicians and participants in the California Cooperative Oceanic Fisheries Investigations program, especially David Wolgast and James Wilkinson, whose dedication and skill made this study possible. We also thank the captains and crews of the R/V *New Horizon*, R/V *Roger Revelle*, and R/V *David Starr Jordan* for their assistance at sea; Mark Haught, Johnny Stutsman, Dave Wilbur, Cynthia Peacock, and Jackie Leung of the University of Washington for their help and expertise in the collection and analysis of O_2 isotope samples; and Suzanne Dickinson and Kathie Kelly of the Applied Physics Laboratory at the University of Washington for processing Quick Scatterometer (QuikSCAT) winds and computing wind stress. Finally, we thank two anonymous reviewers whose insightful comments significantly improved this manuscript.

This work was supported by a University of Washington Program on Climate Change Graduate Fellowship (DRM), a National Defense Science and Engineering Graduate Fellowship (DRM), and National Science Foundation grant Ocean Sciences 0525843 (PDQ).

References

Bakun, A. 1990. Global climate change and intensification of coastal ocean upwelling. Science **247:** 198–201, doi:10.1126/science.247.4939.198

Behrenfeld, M. J., and P. G. Falkowski. 1997. Photosynthetic rates derived from satellite-based chlorophyll concentration. Limnol. Oceanogr. **42:** 1–20, doi:10.4319/lo.1997.42.1.0001

Bograd, S. J., T. K. Chereskin, and D. Roemmich. 2001. Transport of mass, heat, salt, and nutrients in the southern California Current System: Annual cycle and interannual variability. J. Geophys. Res. **106:** 9255–9275, doi:10.1029/1999JC000165

———, C. G. Castro, E. Di Lorenzo, D. M. Palacios, H. Bailey, W. Gilly, and F. P. Chavez. 2008. Oxygen declines and the shoaling of the hypoxic boundary in the California Current. Geophys. Res. Lett. **35:** L12607, doi:10.1029/2008GL034185

Carr, M-E., and others. 2006. A comparison of global estimates of marine primary production from ocean color. Deep-Sea Res. Part II **53:** 741–770, doi:10.1016/j.dsr2.2006.01.028

Chhak, K., and E. Di Lorenzo. 2007. Decadal variations in the California Current upwelling cells. Geophys. Res. Lett. **34:** L14604. , doi:10.1029/2007GL030203

Collins, L. E., W. Berelson, D. E. Hammond, A. Knapp, R. Schwartz, and D. Capone. 2011. Particle fluxes in San Pedro Basin, California: A four-year record of sedimentation and physical forcing. Deep-Sea Res. Part I **58:** 898–914, doi:10.1016/j.dsr.2011.06.008

Craig, H., and T. L. Hayward. 1987. Oxygen supersaturation in the ocean: Biological vs. physical contributions. Science **235:** 199–202, doi:10.1126/science.235.4785.199

Deutsch, C., H. Brix, T. Ito, H. Frenzel, and L. Thompson. 2011. Climate-forced variability of ocean hypoxia. Science **333:** 336–339, doi:10.1126/science.1202422

Di Lorenzo, E., A. J. Miller, N. Schneider, and J. C. McWilliams. 2005. The warming of the California Current: Dynamics and ecosystem implications. J. Phys. Oceanogr. **35:** 336–362, doi:10.1175/JPO-2690.1

Dugdale, R., and F. Wilkerson. 1992. Nutrient limitation of new production in the sea, p. 107–122. *In* p. 107–122, P. G. Falkowski [ed.], Primary productivity and biogeochemical cycles in the sea. Plenum Press.

Dunne, J. P., J. L. Sarmiento, and A. Gnanadesikan. 2007. A synthesis of global particle export from the surface ocean and cycling through the ocean interior and on the seafloor. Glob. Biogeochem. Cycles **21:** GB4006, doi:10.1029/2006GB002907

Emerson, S., P. Quay, D. Karl, C. Winn, L. Tupas, and M. Landry. 1997. Experimental determination of the organic carbon flux from open-ocean surface waters. Nature **389:** 951–954, doi:10.1038/40111

Eppley, R. W. 1992. Chlorophyll, photosynthesis, and new production in the Southern California Bight. Prog. Oceanogr. **30:** 117–150, doi:10.1016/0079-6611(92)90010-W

———, E. Renger, and W. Harrison. 1979. Nitrate and phytoplankton production in southern California coastal waters. Limnol. Oceanogr. **24:** 483–494, doi:10.4319/lo.1979.24.3.0483

Garcia, H. E., and L. I. Gordon. 1992. Oxygen solubility in seawater: Better fitting equations, Limnol. Oceanogr. **37:** 1307–1312.

Grande, K. D., P. J. Williams, J. Marra, D. A. Purdie, K. Heinemann, R. W. Eppley, and M. L. Bender. 1989. Primary production in the North Pacific gyre: A comparison of rates determined by the ^{14}C, O_2 concentration, and ^{18}O methods. Deep-Sea Res. Part I **36:** 1621–1634, doi:10.1016/0198-0149(89)90063-0

Hamme, R. C., and S. E. Emerson. 2004. The solubility of neon, nitrogen and argon in distilled water and seawater. Deep-Sea Res. Part I **51:** 1517–1528, doi:10.1016/j.dsr.2004.06.009

Hendricks, M. B., M. L. Bender, and B. A. Barnett. 2004. Net and gross O_2 production in the Southern Ocean from measurements of biological O_2 saturation and its triple isotope composition. Deep-Sea Res. Part I **51:** 1541–1561, doi:10.1016/j.dsr.2004.06.006

Juranek, L. W., and P. D. Quay. 2005. In vitro and in situ gross primary and net community production in the North Pacific Subtropical Gyre using labeled and natural abundance isotopes of dissolved O_2. Glob. Biogeochem. Cycles **19:** GB3009, doi:10.1029/2004GB002384

———, and ———. 2010. Basin-wide photosynthetic production rates in the subtropical and tropical Pacific Ocean determined from dissolved oxygen isotope ratio measurements. Glob. Biogeochem. Cycles **24:** GB2006, doi:10.1029/2009GB003492

Kahru, M., R. Kudela, M. Manzano-Sarabia, and B. G. Mitchell. 2009. Trends in primary production in the California Current detected with satellite data. J. Geophys. Res. **114:** C02004, doi:10.1029/2008JC004979

———, and B. G. Mitchell. 2002. Influence of the El Niño–La Niña cycle on satellite-derived primary production in the California Current. Geophys. Res. Lett. **29:** 1846, doi:10.1029/2002GL014963

Karl, D. M., J. R. Christian, J. E. Dore, D. V. Hebel, R. M. Letelier, L. M. Tupas, and C. D. Winn. 1996. Seasonal and interannual variability in primary production and particle flux at Station ALOHA. Deep-Sea Res. Part II **43:** 539–568, doi:10.1016/0967-0645(96)00002-1

———, D. V. Hebel, K. Björkman, and R. M. Letelier. 1998. The role of dissolved organic matter release in the productivity of the oligotrophic North Pacific Ocean. Limnol. Oceanogr. **43:** 1270–1286, doi:10.4319/lo.1998.43.6.1270

Knauer, G., and J. Martin. 1981. Primary production and carbon–nitrogen fluxes in the upper 1500 m of the northeast Pacific. Limnol. Oceanogr. **26:** 181–186, doi:10.4319/lo.1981.26.1.0181

Kudela, R. M., and others. 2008. New insights into the controls and mechanisms of plankton productivity in coastal upwelling waters of the northern California Current System. Oceanography **21:** 46–59, doi:10.5670/oceanog.2008.04

Large, W. G., J. C. McWilliams, and S. C. Doney. 1994. Oceanic vertical mixing: A review and a model with a nonlocal boundary-layer parameterization. Rev. Geophys. **32:** 363–403, doi:10.1029/94RG01872

Laws, E. A. 1991. Photosynthetic quotients, new production and net community production in the open ocean. Deep-Sea Res. **38:** 143–167, doi:10.1016/0198-0149(91)90059-O

Luz, B., and E. Barkan. 2000. Assessment of oceanic productivity with the triple-isotope composition of dissolved oxygen. Science **288:** 2028–2031, doi:10.1126/science.288.5473.2028

———, and ———. 2009. Net and gross oxygen production from O_2/Ar, $^{17}O/^{16}O$ and $^{18}O/^{16}O$ ratios. Aquat. Microb. Ecol. **56:** 133–145, doi:10.3354/ame01296

———, and ———. 2011. Proper estimation of marine gross O_2 production with $^{17}O/^{16}O$ and $^{18}O/^{16}O$ ratios of dissolved O_2. Geophys. Res. Lett. **38:** L19606, doi:10.1029/2011GL049138

———, ———, Y. Sagi, and Y. Z. Yacobi. 2002. Evaluation of community respiratory mechanisms with oxygen isotopes: A case study in Lake Kinneret. Limnol. Oceanogr. **47:** 33–42, doi:10.4319/lo.2002.47.1.0033

Marra, J. 1980. Vertical mixing and primary production, p. 121–137. *In* p. 121–137, P. G. Falkowski [ed.], Primary productivity in the sea. Plenum Press.

———. 2002. Approaches to the measurement of plankton production, p. 78–108. *In* p. 78–108, P.J.l.B. Williams, D. N. Thomas, and C. S. Reynolds [eds.], Phytoplankton productivity: Carbon assimilation in marine and freshwater ecosystems. Blackwell.

Messié, M., J. Ledesma, D. D. Kolber, R. P. Michisaki, D. G. Foley, and F. P. Chavez. 2009. Potential new production estimates in four eastern boundary upwelling ecosystems. Prog. Oceanogr. **83:** 151–158, doi:10.1016/j.pocean.2009.07.018

Nicholson, D. P., R. H. R. Stanley, E. Barkan, D. M. Karl, B. Luz, P. D. Quay, and S. C. Doney. 2012. Evaluating triple oxygen isotope estimates of gross primary production at the Hawaii Ocean Time-series and Bermuda Atlantic Time-series study sites. J. Geophys. Res. **117**: C05012, doi:10.1029/2010JC006856

Nightingale, P. D., and others. 2000. In situ evaluation of air–sea exchange parameterizations using novel conservative and volatile tracers. Glob. Biogeochem. Cycles **14:** 373–387, doi:10.1029/1999GB900091

Olivieri, R. A., and F. P. Chavez. 2000. A model of plankton dynamics for the coastal upwelling system of Monterey Bay, California. Deep-Sea Res. Part II **47:** 1077–1106, doi:10.1016/S0967-0645(99)00137-X

Pennington, J. T., G. E. Friederich, C. G. Castro, C. A. Collins, W. W. Evans, and F. P. Chavez. 2010. A carbon budget for the northern and central California coastal upwelling system. Continental Margins Task Team [eds.], The synthesis book. Springer-Verlag.

Prokopenko, M. G., O. M. Pauluis, J. Granger, and L. Y. Yeung. 2011. Exact evaluation of gross photosynthetic production from the oxygen triple-isotope composition of O_2: Implications for the net-to-gross primary production ratios. Geophys. Res. Lett. **38:** L14603, doi:10.1029/2011GL047652

Quay, P. D., C. Peacock, K. Björkman, and D. M. Karl. 2010. Measuring primary production rates in the ocean: Enigmatic results between incubation and non-incubation methods at Station ALOHA. Glob. Biogeochem. Cycles **24:** GB3014, doi:10.1029/2009GB003665

———, J. Stutsman, and T. Steinhoff. 2012. Primary production and carbon export rates across the subpolar N. Atlantic Ocean basin based on triple oxygen isotope and dissolved O_2 and Ar gas measurements. Glob. Biogeochem. Cycles **26:** GB2003, doi:10.1029/2010GB004003

Reid, J. L., and A. W. Mantyla. 1976. The effect of the geostrophic flow upon coastal sea elevations in the northern north Pacific ocean. J. Geophys. Res. **81:** 3100–3110, doi:10.1029/JC081i018p03100

Reuer, M. K., B. A. Barnett, M. L. Bender, P. G. Falkowski, and M. B. Hendricks. 2007. New estimates of southern ocean biological production rates from O_2/Ar ratios and triple isotope composition of O_2. Deep-Sea Res. Part I **54:** 951–974, doi:10.1016/j.dsr.2007.02.007

Robinson, C., and others. 2009. Comparison of in vitro and in situ plankton production determinations. Aquat. Microb. Ecol. **54:** 13–34, doi:10.3354/ame01250

Roemmich, D. 1989. Mean transport of mass, heat, salt and nutrients in southern California coastal waters: Implications for primary production and nutrient cycling. Deep-Sea Res. Part I **36:** 1359–1378, doi:10.1016/0198-0149(89)90088-5

Rykaczewski, R. R., and D. M. Checkley. 2008. Influence of ocean winds on the pelagic ecosystem in upwelling regions. Proc. Natl. Acad. Sci. USA **105:** 1965–1970, doi:10.1073/pnas.0711777105

Sarma, V.V.S.S., O. Abe, and T. Saino. 2008. Spatial variations in time-integrated plankton metabolic rates in Sagami Bay using triple oxygen isotopes and O_2 : Ar ratios. Limnol. Oceanogr. **53:** 1776–1783, doi:10.4319/lo.2008.53.5.1776

Stanley, R. H. R., J. B. Kirkpatrick, N. Cassar, B. A. Barnett, and M. L. Bender. 2010. Net community production and gross primary production rates in the western equatorial Pacific. Glob. Biogeochem. Cycles **24:** GB4001, doi:10.1029/2009GB003651

Stukel, M. R., M. R. Landry, C. R. Benitez-Nelson, and R. Goericke. 2011. Trophic cycling and carbon export relationships in the California Current Ecosystem. Limnol. Oceanogr. **56:** 1866–1878, doi:10.4319/lo.2011.56.5.1866

Thunell, R. C. 1998. Particle fluxes in a coastal upwelling zone: Sediment trap results from Santa Barbara Basin, California. Deep-Sea Res. Part II **45:** 1863–1884, doi:10.1016/S0967-0645(98)80020-9

Westberry, T., M. Behrenfeld, D. Siegel, and E. Boss. 2008. Carbon-based primary productivity modeling with vertically resolved photoacclimation. Glob. Biogeochem. Cycles **22:** GB2024, doi:10.1029/2007GB003078

Zehr, J. P., and R. M. Kudela. 2009. Photosynthesis in the open ocean. Science **326:** 945–946, doi:10.1126/science.1181277

Associate editor: Robert R. Bidigare

Received: 24 August 2012
Accepted: 16 January 2013
Amended: 22 March 2013